THE JOURNAL OF COMPARATIVE NEUROLOGY 427:67–92 (2000)

Expression of Calcium-Binding Proteins in the Diencephalon of the Lizard *Psammodromus algirus*

JOSÉ CARLOS DÁVILA,[1] SALVADOR GUIRADO,[1]* AND LUIS PUELLES[2]
[1]Departamento de Biología Celular, Universidad de Málaga, 29071 Málaga, Spain
[2]Departamento de Ciencias Morfológicas, Universidad de Murcia, 30100 Murcia, Spain

ABSTRACT

This work is a study of the distribution pattern of calbindin-D28k, calretinin, and parvalbumin in the diencephalic alar plate of a reptile, the lizard *Psammodromus algirus*, by using the prosomeric model (Puelles [1995] Brain Behav Evol 46:319–337), which divides the alar plate of the diencephalon into the caudorostrally arranged pretectum (p1), dorsal thalamus plus epithalamus (p2), and ventral thalamus (p3). Calbindin and calretinin are more extensively expressed in the dorsal thalamus than in the neighboring alar regions, and therefore these calcium-binding proteins are particularly suitable markers for delimiting the dorsal thalamus/epithalamus complex from the ventral thalamus and the pretectum. Conversely, parvalbumin is more intensely expressed in the pretectum and ventral thalamus than in the dorsal thalamus/epithalamus complex. Within the dorsal thalamus, calcium-binding protein immunoreactivity reveals a three-tiered division. The pretectum displays the most intense expression of parvalbumin within the diencephalon. Virtually all nuclei in the three sectors of the pretectum (commissural, juxtacommissural, and precommissural) present strong to moderate expression of parvalbumin. We compare the distribution of calcium-binding proteins in the diencephalon of *Psammodromus* with other vertebrates, with mammals in particular, and suggest that the middle and ventral tiers of the reptilian dorsal thalamus may be comparable to nonspecific or plurimodal posterior/intralaminar thalamic nuclei in mammals, on the basis of the calcium-binding protein expression patterns, as well as the hodological and embryological data in the literature. J. Comp. Neurol. 427:67–92, 2000.

Indexing terms: calbindin; parvalbumin; calretinin; comparative neuroanatomy; reptile

Although a wealth of data is available on the organization of the thalamus in mammals, there are comparative aspects about the structure and function of the thalamus of vertebrates which remain poorly understood. The traditional interpretation (e.g., as reviewed by Jones, 1985; Butler, 1995) is that most thalamic nuclei are identified and named according to their topography in cross-sections; this interpretation schema is based on the recently challenged "columnar paradigm" assumptions of Herrick (1910, 1948). In contrast, there is scanty information on the topology of these nuclei relative to neuromeric developmental coordinates, emphasized in recent works (Puelles, 1995; Shimamura et al., 1995; Nieuwenhuys, 1998; Redies et al., 2000), or on the histogenetic complexes which precede their constitution during development. These kinds of data are particularly lacking for the reptilian thalamus, yet an understanding of thalamic organization in reptiles is essential for testing theories about the evolution of the more complex avian and mammalian diencephalic patterns, and, further, for theories of telencephalic evolution. Apart from a few cytoarchitectonic studies on the reptilian diencephalon performed recently (Butler and Northcutt, 1973; Cruce, 1974; Senn, 1979; Hergueta et al., 1993), there has been only limited work on analyzing its structure (Pritz and Stritzel, 1986, 1988, 1990; Díaz et al., 1994; Pritz, 1995, 1997; Pritz and Siadati, 1999). Moreover, most recent studies on the reptilian thalamus deal with the extrinsic connectivity of the dorsal

Grant sponsor: Spanish DGES; Grant number: PB96-0715; Grant sponsor: Spanish DGICYT; Grant number: PB98-397.

*Correspondence to: Dr. S. Guirado, Depto. Biología Celular, Facultad de Ciencias, Campus de Teatinos, 29071 Málaga, Spain.
E-mail: guirado@uma.es

Received 11 February 2000; Revised 10 July 2000; Accepted 10 July 2000

thalamus and especially with the visual thalamus (Dacey and Ulinski, 1983; Pritz and Stritzel, 1992; Kenigfest et al., 1997; Martinez-Marcos et al., 1998), whereas other "thalamic" regions, such as the ventral thalamus, the epithalamus, or the pretectum, are not addressed in detail. Exceptions to this are the studies of Pritz and Stritzel (1990) and Díaz et al. (1994) on the reptilian reticular nucleus in the ventral thalamus.

Very few chemoarchitectonic studies have focused on specific nuclei of the reptilian diencephalon (Brauth et al., 1988; Rio et al., 1992; Pritz and Stritzel, 1994; Kenigfest et al. 1995, 1997; Pritz and Siadati, 1999), so that available chemoarchitectonic data on the reptilian diencephalon are few and incomplete. In fact, they have been obtained mainly from studies of the distribution pattern of neurotransmitter or neuropeptide markers in the whole brain of a limited number of species (i.e., γ-aminobutyric acid [GABA] in *Chamaleo*: Bennis et al., 1991; neuropeptide Y [NPY] and choline acetyltransferase [ChAT] in *Gallotia*: Medina et al., 1992, 1993).

One aim of the present work is to provide a comprehensive study of the distribution pattern of calbindin-D28k (CB), calretinin (CR), and parvalbumin (PV) in the diencephalon of the lacertid lizard *Psammodromus algirus*, a species in which we already studied a number of cyto- and chemoarchitectonic aspects in the telencephalon (Dávila et al., 1991, 1993, 1995, 1997, 1999; Guirado et al., 1999). These calcium-binding proteins are highly conserved in vertebrates and have been shown to be useful morphological markers that label specific neurons or circuits in brains of both mammals (Celio and Heizmann, 1981; Jones and Hendry, 1989; Hendry et al., 1989; Celio, 1990; Andressen et al. 1993) and nonmammalian vertebrates (Braun, 1990; Dávila et al., 1993, 1997, 1999; De Castro et al., 1998; Guirado et al., 1999; Milán and Puelles, 2000).

Here we studied the distribution of calbindin-D28k, calretinin, and parvalbumin in serial sections of the lizard diencephalon, by using as a framework the prosomeric model (Puelles, 1995). In this model, the diencephalon is divided into three prosomeres p1–p3, which contain, respectively, the pretectum, the dorsal thalamus/epithalamus complex, and the ventral thalamus as alar regions, and the prerubral tegmentum, the posterior tuberculum area, and the retromammillary area as the corresponding basal plate sectors. Secondly, we aimed to compare the distribution of these markers in a lizard with the patterns found in other vertebrates (i.e., Pombal and Puelles, 1999; Milán and Puelles, 2000), and with mammals in particular. In view of recent work from our laboratory regarding connections of the thalamic nucleus rotundus (Guirado et al., 2000), we also wanted to examine the hypothesis that tectorecipient thalamic neuronal populations of sauropsids may be field homologs of mammalian posterior and intralaminar nuclei, in the light of our findings and published data concerning chemoarchictectural, hodological, and functional characteristics of the mammalian dorsal thalamus.

MATERIALS AND METHODS

Adult lizards of the species *Psammodromus algirus* (Lacertidae) were used in the present study. Throughout the

ABBREVIATIONS

ac	anterior commissure
AI	area intercalata
AT	area triangularis
bpt	basal plate tracts
BSM	bed nucleus of the stria medullaris
Cer	cerebellum
CM	caudomedial nucleus
Ctx	cerebral cortex
DLA	dorsolateral anterior nucleus
DLC	dorsolateral caudal nucleus
DLH	dorsolateral hypothalamic nucleus
DLP	dorsolateral posterior nucleus
DM	dorsomedial nucleus
DT	dorsal thalamus
DVR	dorsal ventricular ridge
EMT	eminentia thalami
fb	forebrain bundle
GD	dorsal geniculate nucleus
GP	pretectal geniculate nucleus
GT	griseum tectale
GV	ventral geniculate nucleus
HL	lateral habenular nucleus
HMd	medial habenular nucleus, dorsal portion
HMv	medial habenular nucleus, ventral portion
Hyp	hypothalamus
IGL	intergeniculate leaflet formation
IM	intermediomedial nucleus
IPCm	interstitial nucleus of the posterior commissure, pars magnocellularis
IPCp	interstitial nucleus of the posterior commissure, pars parvocellularis
JCL	lateral juxtacommissural nucleus
JCM	medial juxtacommissural nucleus
lfb	lateral forebrain bundle
M	medial thalamic nucleus
O	nucleus ovalis
OT	optic tectum
ot	optic tract
p1–p6	prosomeres 1–6
pac	pallial commissure
PAG	periacueductal grey
pc	posterior commissure
PCSV	posterior nucleus of the commissura supraoptica ventralis
PD	posterodorsal nucleus
PE	external pretectal nucleus
PL	posterolateral nucleus
PM	posteromedial nucleus
POA	preoptic area
PP	principal pretectal nucleus
PPC	principal precommissural nucleus
PrM	medial pretectal nucleus
PT	pretectum
R	nucleus rotundus
RM	retromammillary region
RSa	rotundic shell anterior
RSp	rotundic shell posterior
RSv	rotundic shell ventral
rt	retroflex tract
SCL	lateral suprachiasmatic nucleus
sco	subcommissural organ
SHl	lateral subhabenular area
SHm	medial subhabenular area
SHr	rostral subhabenular nucleus
sm	stria medullaris
SP	subpretectal nucleus
VL	ventrolateral nucleus
VM	ventromedial nucleus
VT	ventral thalamus
Z	nucleus Z
zl	zona limitans intrathalamica
II	optic nerve
III	oculomotor nerve

experimental work, the lizards were treated according to the European Communities Council Directive (86/609/EEC) on treatment of experimental animals.

Lizards were deeply anesthetized with urethane and transcardially perfused with 0.1 M phosphate-buffered saline (PBS), pH 7.4, followed by 4% paraformaldehyde, 0.1% glutaraldehyde, and 0.2% picric acid in PBS at room temperature for 30 minutes. The brains were then removed and stored in 4% paraformaldehyde and 0.2% picric acid in PBS at 4°C overnight; afterwards they were embedded in 4% agar and cut into 50-μm-thick sections, by using a vibratome. Both frontal and sagittal sections series were prepared. The sections were washed extensively in PBS prior to immunocytochemical staining with the peroxidase-antiperoxidase method.

Free-floating sections were first incubated in 2% normal goat serum and 0.3% Triton X-100 in PBS at room temperature for 1 hour, to block nonspecific binding of the antibodies and permeate the tissues, respectively, and then were transferred to the primary antibody. The three polyclonal antibodies, anti-PV, anti-CR, and anti-CB, were raised in rabbits (SWant, Bellinzona, Switzerland) and used at a dilution of 1:2,000 for 18 hours. After three washes in PBS for 45 minutes, the sections were incubated in goat anti-rabbit IgG diluted 1:35 for 1 hour, washed again in PBS for 45 minutes, and incubated in peroxidase-antiperoxidase diluted 1:100 for 1 hour. The immunolabeling was revealed with 0.05% diaminobenzidine (DAB), 0.05% nickel ammonium sulfate and 0.03% hydrogen peroxide (H_2O_2) in PBS. All steps were carried out at room temperature with gentle agitation. After a thorough wash in PBS, the sections were mounted onto gelatinized slides, air-dried, dehydrated in ethanol, cleared in xylene, and coverslipped with DPX.

Controls

As controls of the immunohistochemical method used in the present study, sections were processed as indicated but the corresponding primary antiserum was replaced by rabbit nonimmune serum (1:500). No immunostaining could be detected under these conditions. In addition, as a control of the specificity of the different primary antisera under the experimental conditions used in this work, we incubated control sections in the primary antibody preadsorbed with the corresponding protein (1 μg per ml of the diluted antibody). As a result, specific immunostaining was completely abolished.

RESULTS

We group our data below into brain regions, in order to aid comparison among the three sets of immunochemical results for each structural complex. The schema for subdivisions follows the prosomeric model (Martinez-de-la-Torre, 1985; Medina et al., 1993, 1994; Puelles, 1995; Puelles et al., 1996), which divides the diencephalon into three prosomeres (p1–p3), numbered in caudorostral order (Fig. 1). We shall concentrate on the respective alar regions of p1–p3, corresponding to the pretectum (p1), the dorsal thalamus plus epithalamus (p2), and the ventral thalamus (p3). The basal plate regions need a separate study by themselves, because they never have been analyzed in much detail within a segmental paradigm. Preliminary observations do suggest differences related to prosomeric position, as well as some common traits. A first effort to systematize segmentally the diencephalic basal plate of human embryos was finished recently (Verney et al., unpublished observations; see also Medina et al.,1994; Puelles and Medina,1994). The hypothalamus falls outside of the diencephalon proper in the prosomeric model (basal part of the secondary prosencephalon, that is, p4–p6; Puelles, 1995) and will not be addressed in the present description.

Overview

Alar and basal regions of the lizard diencephalon can be easily distinguished in selected sagittal sections on the basis of cytoarchitectural differences and myeloarchitecture (Fig. 1A,B). The midbrain-diencephalon boundary passes just caudal to the fibers of the posterior commissure (Palmgren, 1921; Rendahl, 1924). Ventrally it continues rostral to the red nucleus and oculomotor root (Fig. 1). The transverse boundary between the diencephalon and the secondary prosencephalon (p3/p4 limit) passes in front of the ventral thalamus, slightly behind the lateral and medial forebrain bundles coursing in the preoptopeduncular region (p5) and just behind the paraventricular and suprapeduncular nuclei and the mammillary pouch (p4). The p1/p2 transverse boundary starts at the dorsal midline at the joint rostral end of the posterior commissure and the subjacent subcommissural organ (not seen in Fig.1). More ventrally, this boundary gradually approaches the retroflex tract, which further ventrally serves as a constant landmark, just rostral to the boundary, down to the floor region (Fig. 1). Finally, the p2/p3 boundary, or zona limitans intrathalamica, neatly separates dorsal thalamus from ventral thalamic grisea all the way from the diencephalic roof to the alar-basal limit, and can be extrapolated across the basal plate into the tuberculum posterior at the apex of the cephalic flexure (Fig. 1). The basal plate sectors corresponding to each neuromere correlate with the prerubral tegmentum (p1), the posterior tuberculum area (p2), and the retromammillary area (p3).

As shown in Figure 3, the calbindin- and calretinin-immunostained material underlines these main subdivisions, at least in the alar plate, insofar as numerous neuronal populations of the dorsal thalamus (p2) are immunoreactive for these markers, whereas fewer CB-immunoreactive (IR) or CR-IR populations are found in the pretectum (p1) or in the ventral thalamus (p3). Conversely, parvalbumin immunostaining largely underlines the pretectal and ventral thalamic grisea, though some dorsal thalamic ones also express this marker (Fig. 3).

In the following description of results, we deal first with the epithalamus and dorsal thalamus and later with the ventral thalamus and pretectum. In each case, further details of morphologic subdivision precede the chemoarchitectural data.

Epithalamus

The epithalamus consists of the epiphysis and the habenular complex. The latter has a compact, partly asymmetric medial habenular nucleus and a lateral habenular nucleus (HM, HL; Fig. 2B,C). The HL is more extensive rostrally, where it appears as loosely distributed cells interstitial to the fibers of the stria medullaris (HL; Fig. 2B); caudally, HL is represented by a few cells in the same interstitial position (Fig. 2C). The HM nucleus consists of a symmetric ventral portion (HMv) and an asymmetric

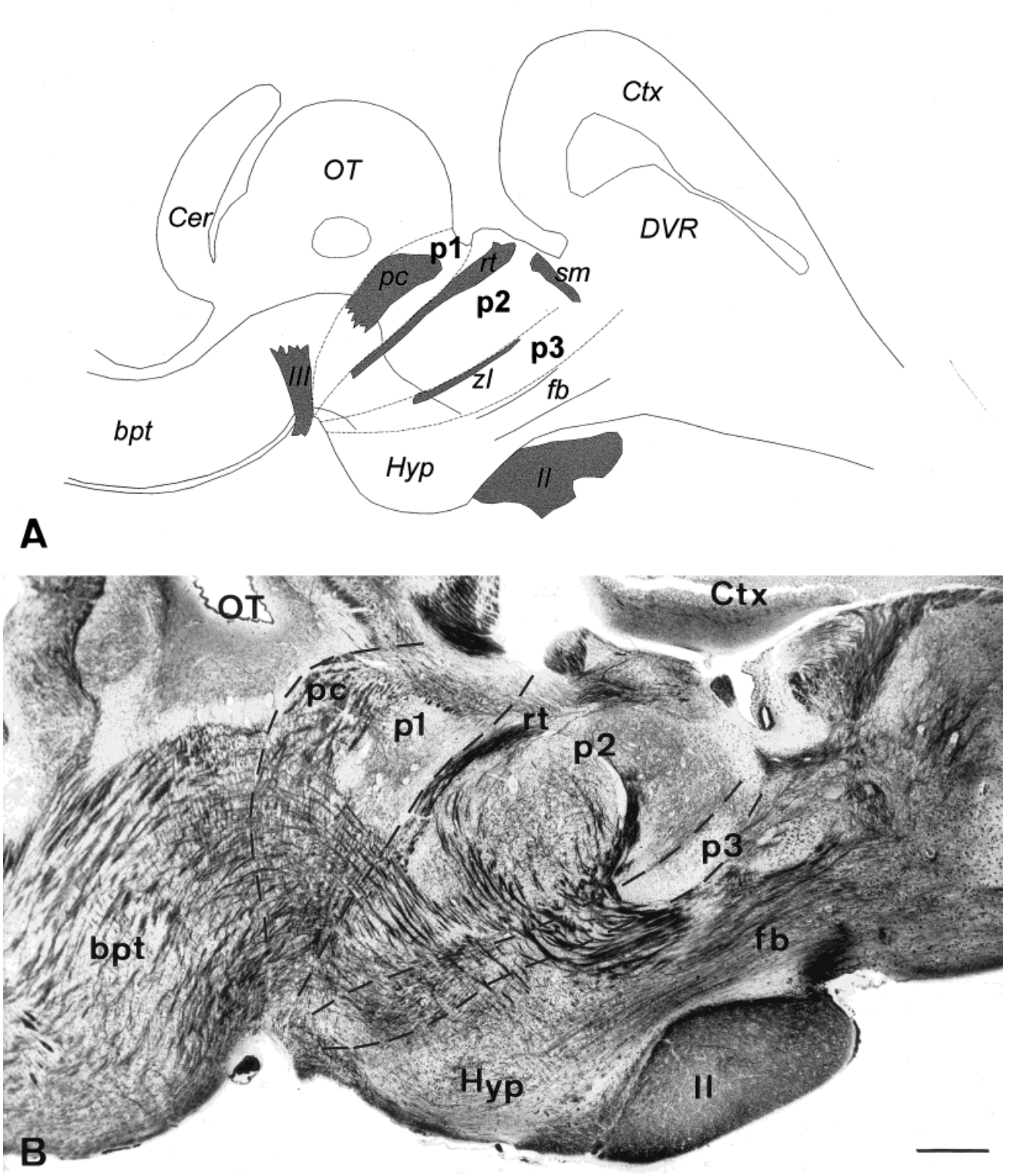

Fig. 1. Overview of the diencephalon of *Psammodromus*. **A:** Schematic drawing of a sagittal section of the brain showing the main divisions of the diencephalon, as proposed in the prosomeric model (Puelles, 1995; see text for explanation). **B:** Sagittal section of the brain of *Psammodromus* stained with the reduced silver nitrate method of Cajal. The main myelinated fiber tracts and the boundaries of the p1–p3 prosomeres are marked. For abbreviations in this and subsequent figures, see list. Scale bar = 200 μm.

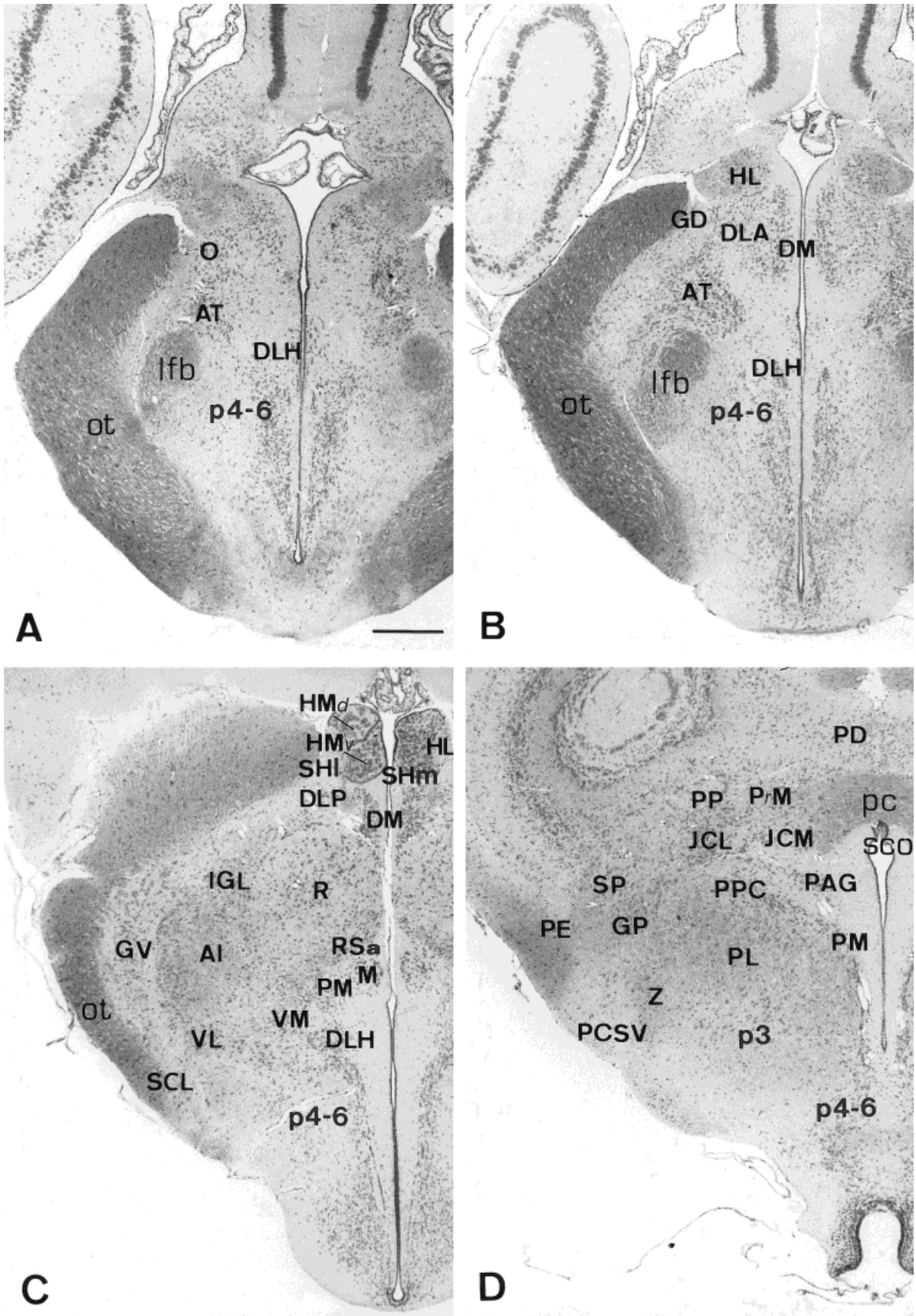

Fig. 2. **A–D:** Selected Nissl-stained frontal sections through the diencephalon of *Psammodromus*. Sections are rostrocaudally arranged (A, rostralmost; D, caudalmost). The majority of nuclei in the dorsal and ventral thalamus, as well as in the pretectum are marked. Scale bar = 250 μm.

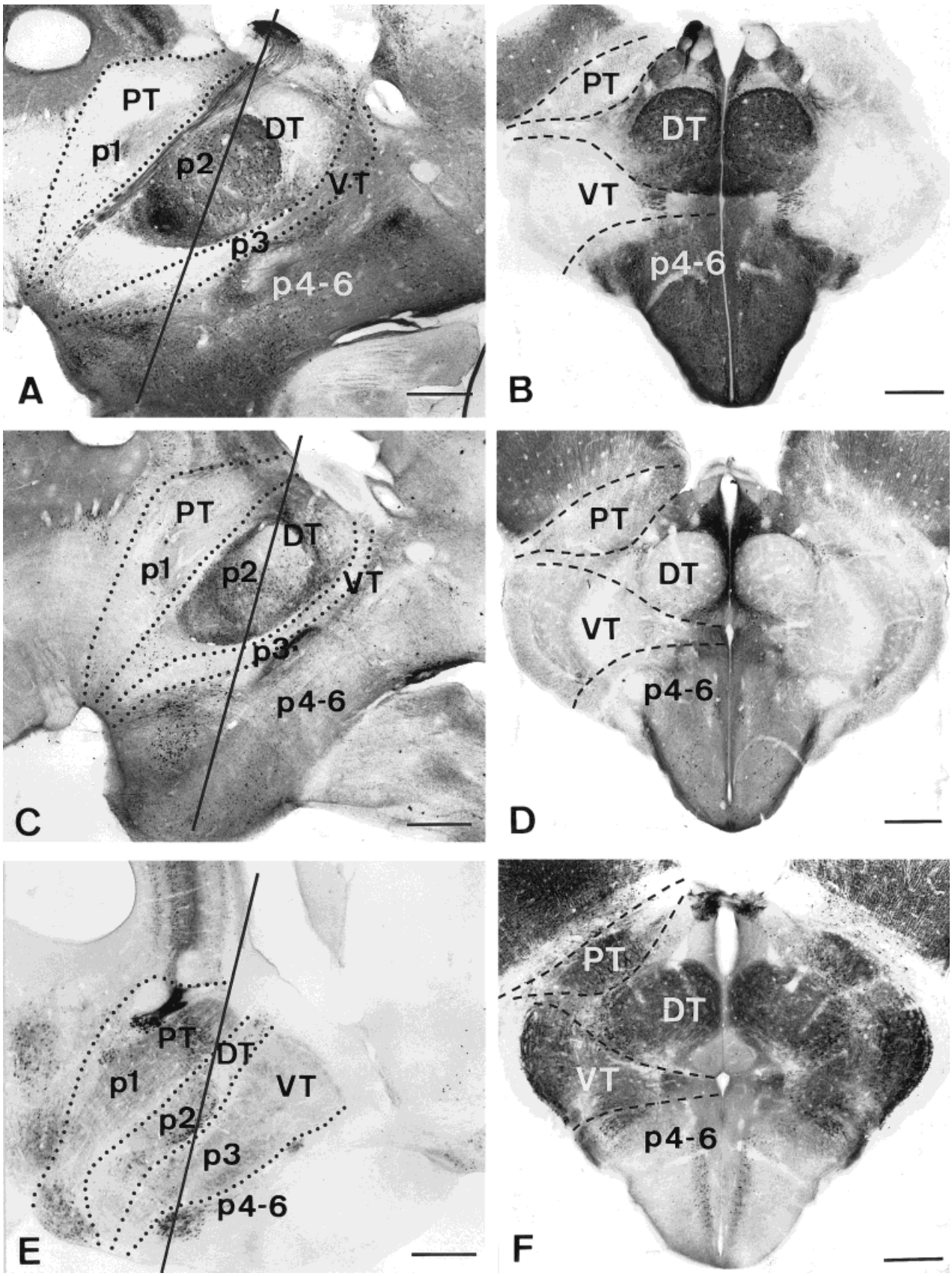

Fig. 3. Overall distribution of the three calcium-binding proteins (calbindin: **A,B**; calretinin: **C,D**; parvalbumin: **E,F**) in the diencephalon of *Psammodromus* as seen in sagittal (A,C,E) and frontal (B,D,F) sections. The boundaries of the p1–p3 prosomeres are marked by dotted lines. The solid line in A, C, and E represents the level of cross-section in B, D, and F, respectively. Scale bars = 300 μm.

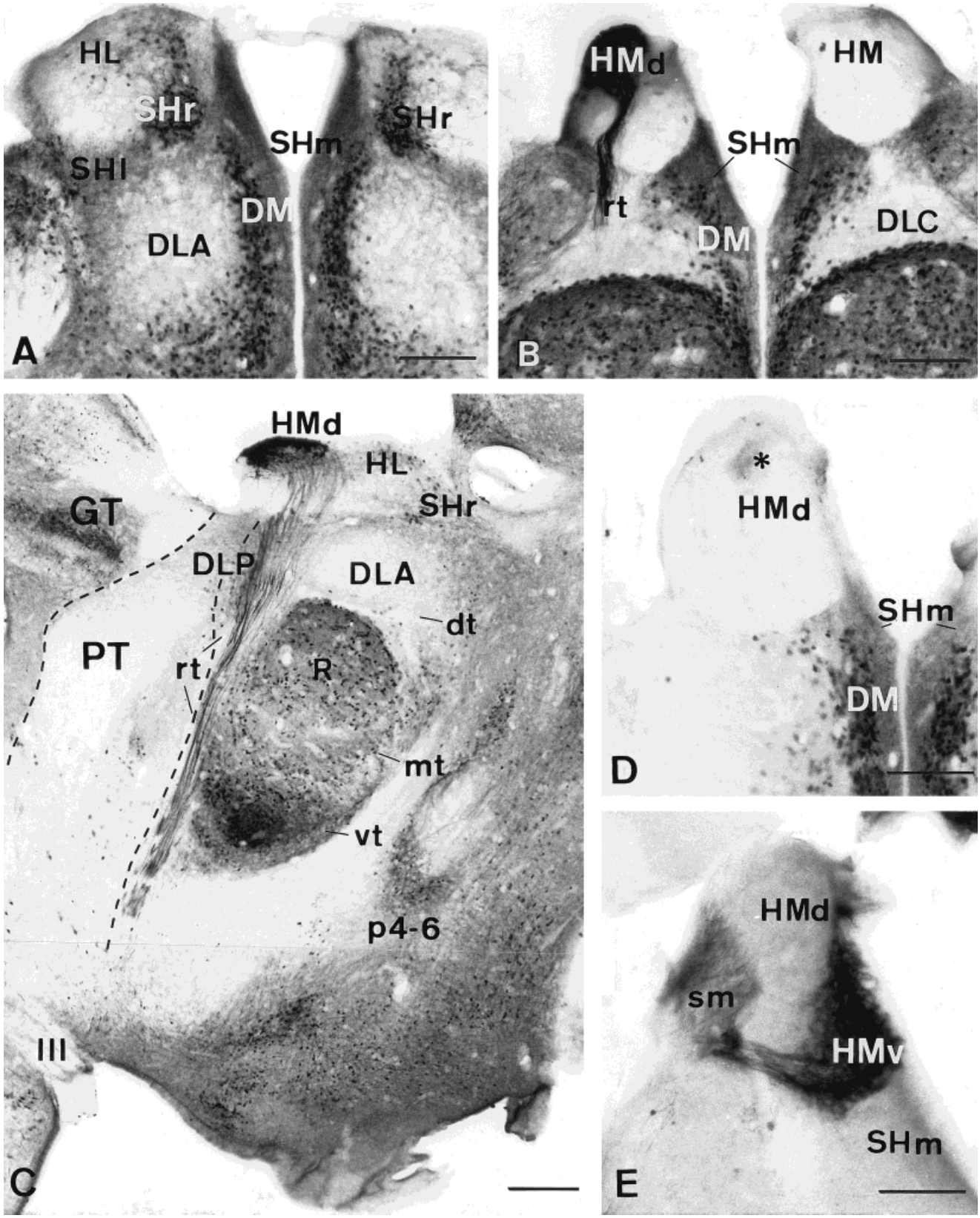

Fig. 4. Immunoreaction pattern of calcium-binding proteins in the epithalamus. **A:** Detail of the dorsalmost portion of the dorsal thalamus in a frontal section of the brain stained with anti-calbindin antibody. Numerous calbindin-D28k-immunoreactive (CB-IR) neurons can be seen in the rostral subhabenular nucleus bilaterally (SHr). **B:** Calbindin immunostaining in the epithalamus. Frontal section, caudal to A. Note the asymmetric presence of intense CB immunoreactivity in the dorsal part of the left medial habenular nucleus (HMd). **C:** Calbindin immunoreactivity in a sagittal section through the diencephalon, showing the course of the immunoreactive retroflex tract (rt), bordering the dorsal thalamus-pretectum limit (pretectum limits are defined by dashed lines). Note the three-tiered structure of the dorsal thalamus (dt,mt,vt: dorsal, middle, and ventral tiers, respectively). **D:** Calretinin immunoreactivity in the epithalamus. Only the dorsal part of the left medial habenular nucleus (HMd) displays a few barely distinguishable immunoreactive neurons (asterisk). **E:** Parvalbumin immunoreactivity in the epithalamus. The epithalamus lacks parvalbumin-reactive (PV-IR) neurons but displays a dense immunoreactive plexus in the ventromedial portion of the medial habenular nucleus (HM). Scale bars = 125 μm in A,B; 200 μm in C; 100 μm in D,E.

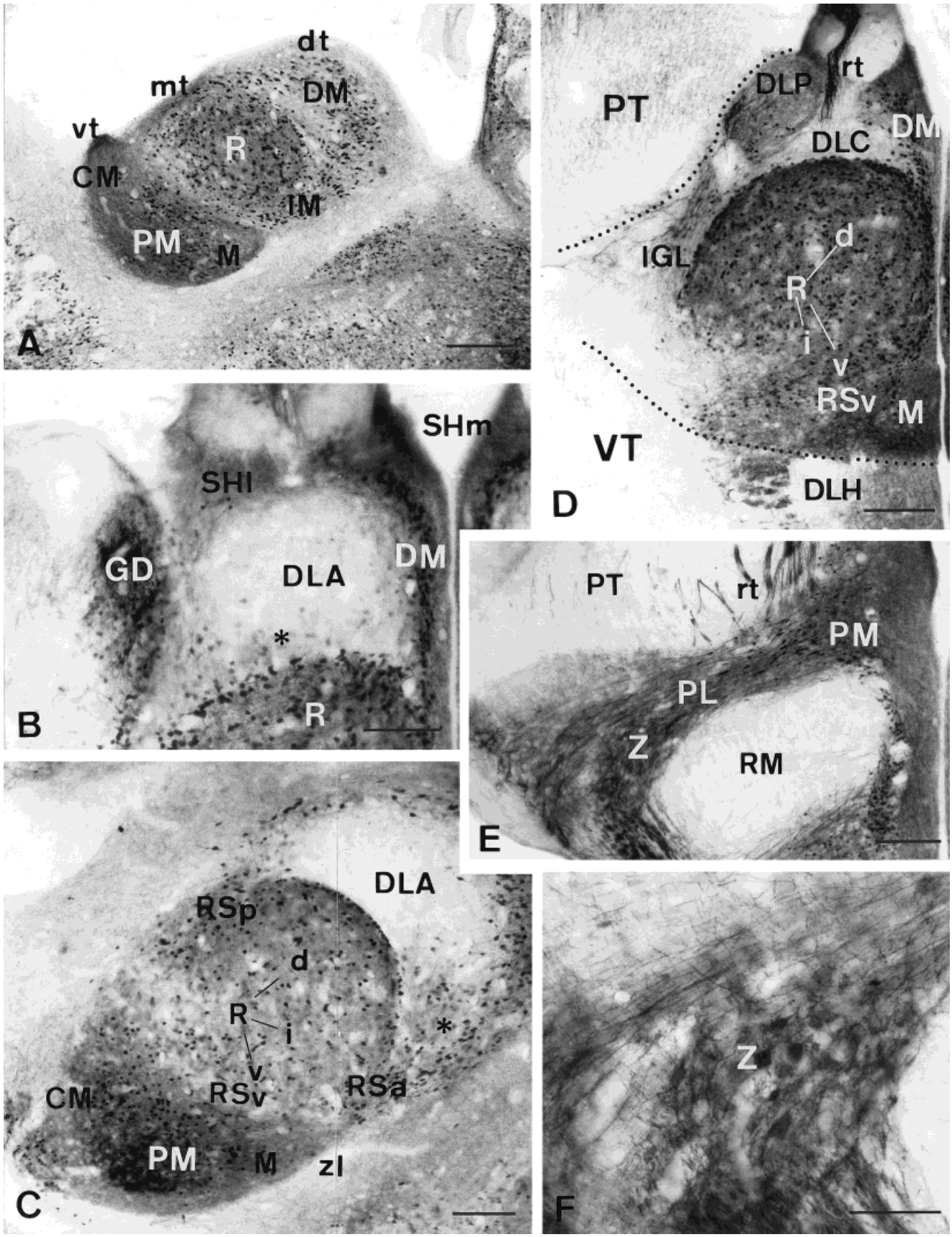
dt
mt
DM
vt
R
CM
IM
PM
M
A
PT
DLP
rt
DLC
DM
IGL
d
R
i
v
RSv
M
VT
DLH
D
SHm
SHl
GD
DLA
DM
*
R
B
PT
rt
PM
PL
Z
RM
E
DLA
RSp
d
R
i
v
*
CM
RSv
RSa
PM
M
zl
C
Z
F

Figure 5

dorsal portion (HMd). The latter appears at the left side of the brain, and is characterized by neurons that adhere to one another in a peripheral capsule, plus several inner cell clumps or laminae, leaving cell-free areas of neuropil (Fig. 2C). Ventral to the habenular complex, small cell-poor regions constitute the medial and lateral subhabenular areas (SHm, SHl; Fig. 2C); there also seems to exist a separate rostral subhabenular nucleus, as suggested by differential immunostaining reported below (SHr; Fig. 4A,C). The subhabenular nuclei are conventionally treated as part of the habenular complex. However, they have a distinct limit with the habenular nuclei, whereas their limit with underlying dorsal thalamic grisea is indistinct. Moreover, they do not project through the retroflex tract (Diaz and Puelles, 1992a), which suggests that they may rather belong to the dorsal thalamus. They are therefore treated under that heading below.

Calbindin. The lateral habenular nucleus presents rostrally a number of weakly CB-IR neurons (HL; Fig. 4A,C). The medial habenular nucleus shows an asymmetric expression pattern (Fig. 4B). At the right, the whole HM nucleus is negative for CB. In contrast, the cytoarchitectonically distinct dorsal subdivision in the left HM nucleus is intensely CB-IR (HMd; Figs. 3C, 4B). The HMd cells extend CB-IR axons into the retroflex tract in the form of several separate fascicles (rt; Figs. 4C, 5E, 9A). These can be followed down to the floor of the diencephalon, always in front of the p1/p2 boundary (Fig. 4C). Afterwards the whole tract takes a longitudinal course caudalwards, into the interpeduncular nucleus (Diaz and Puelles, 1992a).

Calretinin. Calretinin immunostaining in the epithalamus is restricted to a number of very weakly CR-IR neurons in the asymmetric left HMd, in the same position occupied by CB-IR neurons (asterisk in Fig. 4D); however, no CR-immunostained axon can be followed into the ipsilateral retroflex tract; this result may represent cross-reaction of the anti-calretinin antibody in the presence of highly concentrated CB (compare Fig. 4B).

Parvalbumin. Fibers of the stria medullaris are moderately PV-IR as they cross longitudinally the epithalamus, approaching the habenular commissure; they may originate in the nucleus of the posterior pallial commissure, which is intensely PV-IR (not shown; see Diaz and Puelles, 1992b). Terminals or collaterals from these fibers enter the medial habenular nucleus along its length, passing just over the epithalamo/dorsal thalamus boundary, and generating a dense PV-IR plexus in the medial part of its symmetric ventral portion (HMv; Fig. 4E).

Dorsal thalamus

The nuclear structure of the dorsal thalamus can be subdivided for systematic purposes into three dorsoventrally disposed tiers (dt, mt, vt; Figs. 4C, 5A,C, 6A; see also Martínez-de-la-Torre, 1985; Diaz et al., 1994; Pombal and Puelles, 1999; Redies et al., 2000). Note that the dorsoventral axis employed here for defining the three superposed tiers is that of the segmental paradigm (Puelles, 1995), which is parallel to the transverse retroflex tract (Fig.1). Neuroanatomists using the conventional columnar paradigm would tend to interpret our ventral tier as a "posterior" part of the dorsal thalamus. The *dorsal tier* contains the rostral, medial, and lateral subhabenular nuclei, the dorsal, thicker portion of the dorsomedial nucleus, and the chemoarchitectonically distinct anterior and caudal dorsolateral nuclei, plus the dorsal geniculate nucleus, which lies superficially within this tier, and a small dorsocaudal area just behind the habenular nuclei. The dorsal tier thus includes most of the conventional "dorsal" nuclei (Fig. 2B,C). The *middle tier* expands into the roof of the diencephalon, caudal to the dorsal tier and epithalamus, and it mainly contains the posterior dorsolateral nucleus and the rotundus complex (rotundus core and shell; Figs. 2C, 4C), plus the associated periventricular stratum, formed by the ventral thinner part of the dorsomedial nucleus, or intermediomedial nucleus (see below). The perirotundic portion of the intergeniculate leaflet formation covers superficially the middle tier. The *ventral tier* contains the medial, caudomedial, posteromedial, and posterolateral nuclei, as well as other less well-known formations, such as nucleus Z, nucleus ansa lenticularis posterior, and the posterior nucleus of the ventral supraoptic commissure (Fig. 2C,D).

Calbindin. Just under the epithalamus, CB-IR cells appear bilaterally in a rostral dense group of neurons lying just at the rostrodorsal border of the dorsal thalamus, as defined above. This nucleus is structurally and chemoarchitectonically distinct from the conventional, cell-poor, lateral and medial subhabenular nuclei found more caudally. We therefore introduce the term "rostral" subhabenular nucleus for this population (SHr; Fig. 4A,C). These cells are flanked by CB-IR neuropil areas, which we identify as the medial and lateral subhabenular areas, respectively (SHm, SHl; Fig. 4A,B). The SHm is periventricular and displays an intensely CB-IR neuropil, as well as some positive cells; it is in contact with the dorsomedial nucleus ventrally. The SHl lies laterally, where it reaches the brain surface below the stria medullaris tract (a subpial landmark identifying the ventral

Fig. 5. Calbindin immunoreactivity in the dorsal thalamus. **A:** Paramedian sagittal section showing the dorsoventral tiered arrangement of nuclei in the dorsal thalamus (dt, mt, vt: dorsal, middle, and ventral tiers, respectively). **B:** Detail of the dorsal tier in a frontal section. The dorsolateral anterior nucleus (DLA) is almost immunonegative with the exception of its ventral region (asterisk), in contrast to both the dorsomedial (DM) and dorsal geniculate (GD) nuclei that display calbindin-D28k-immunoreactive (CB-IR) neurons and neuropil. **C:** Sagittal section through the diencephalon. In the middle tier, various subdivisions can be clearly distinguished in the rotundic complex. In the ventral tier, the medial, posteromedial, and caudomedial nuclei (M, PM, CM) stand out by their strong CB-IR. The asterisk marks the ventral portion of DLA. **D:** Frontal section at the caudal end of the dorsal tier. In the dorsal tier, the dorsolateral caudal nucleus (DLC) appears near the retroflex tract (rt); in the middle tier, the dorsolateral posterior nucleus (DLP) and the nucleus rotundus (R) can be observed (dorsal thalamus limits are defined by dotted lines). **E:** Lateral derivatives of the ventral tier at caudal levels of the dorsal thalamus, near the basal plate. This region displays a high CB immunoreactivity, in contrast to the overlying pretectum (PT) and the underlying ventral thalamic basal plate (retromammillary region, RM). **F:** Detail of the nucleus Z, showing moderately immunostained large neurons embedded in a reactive neuropil. Scale bars = 200 μm in A; 75 μm in B,F; 125 μm in C,D; 150 μm in E.

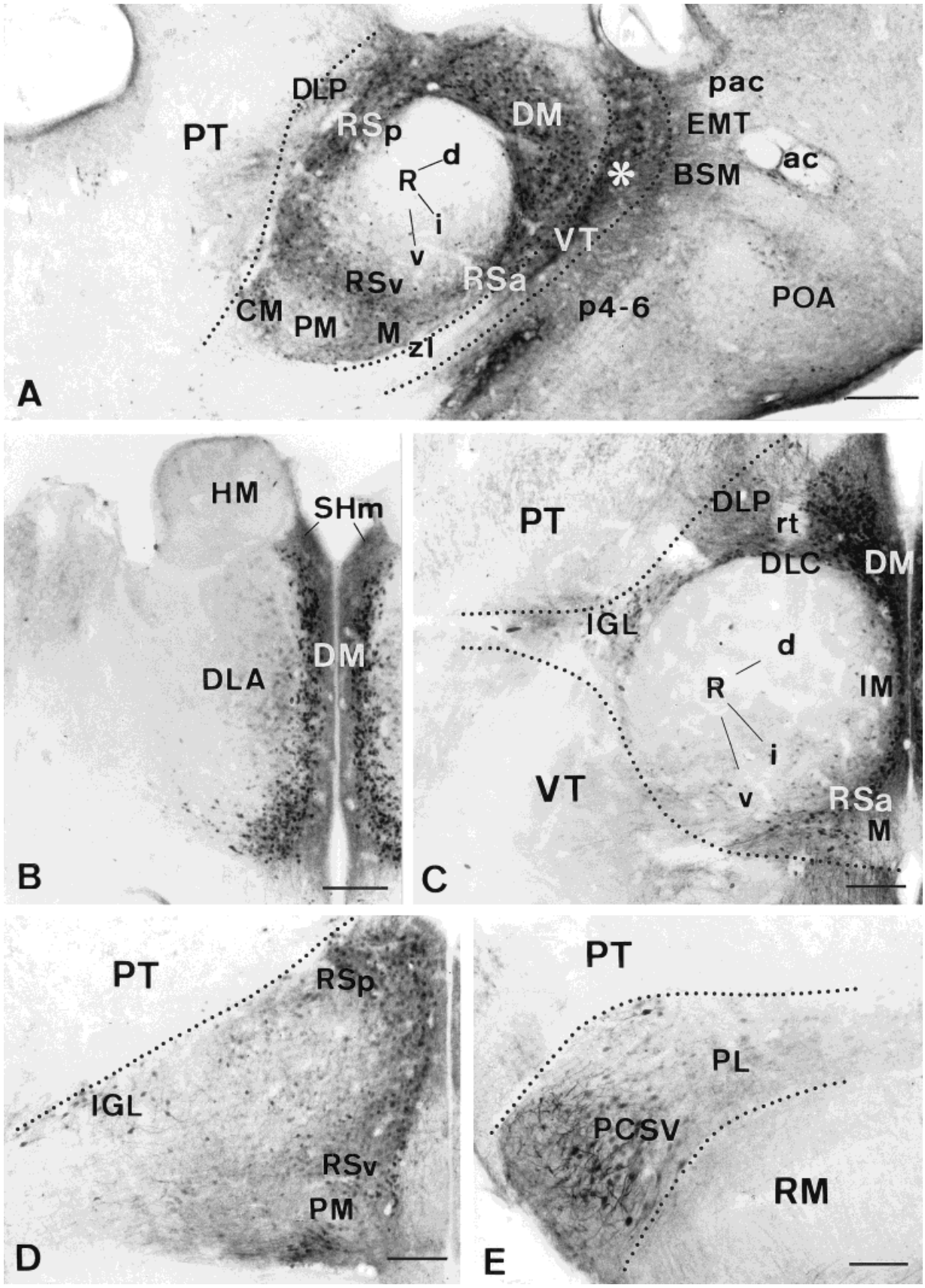
DLP
PT
RSp
DM
pac
EMT
d
R
*
BSM
ac
i
v
VT
RSv
RSa
CM
PM
M
zl
p4-6
POA
A
HM
SHm
DM
DLA
B
PT
DLP
rt
DLC
DM
IGL
d
R
IM
i
VT
v
RSa
M
C
PT
RSp
IGL
RSv
PM
D
PT
PL
PCSV
RM
E

Figure 6

border of the epithalamus); its CB-IR neuropil is less dense than that of SHm. The dorsomedial nucleus (dorsal part) is uniformly CB-IR; that is, both its neurons and neuropil are strongly immunoreactive (DM; Fig. 5A,B,D). Conversely, the dorsolateral anterior nucleus is practically devoid of CB signal, with the exception of its ventral, suprarotundic region, where sparse weakly immunoreactive neurons were found (DLA; asterisk in Fig. 5B,C). In contrast, the dorsal geniculate nucleus has numerous CB-IR cells in the deep cell plate and a CB-IR neuropil (GD; Fig. 5B).

In the middle tier, the nucleus rotundus is massively CB-IR (many neurons and neuropil), with particularly strong signal in the perirotundal capsule (R; Figs. 4C, 5A–D). Sagittal and transverse sections (see also other markers below) illustrate that the rotundic core region is heterogeneous chemoarchitectonically, so that a large dorsal part is separated from a smaller ventral part by a thin intermediate area. The latter is relatively poor in CB-IR neurons (Rd, Ri, Rv; Fig. 5C,D). The posterior, ventral, and anterior rotundic shell regions represent additional cell populations surrounding the rotundic core. The posterior and anterior rotundic shell populations also contain many CB-IR cells, whereas the ventral rotundic shell appears as a CB-negative gap that separates the rotundic complex from the underlying ventral tier formation (RSp, RSa, RSv; Fig. 5C,D). The posterior dorsolateral nucleus, which lies at the dorsocaudal end of the middle tier, separating the pretectum from the thalamic dorsal tier and epithalamus, shows some CB-immunoreactive neurons and a moderately CB-IR neuropil (DLP; Figs. 4C, 5D). The periventricular stratum corresponding to the middle tier is formed by a slightly distinct, thinner ventral portion of the conventional dorsomedial nucleus, which we propose can be distinguished as the intermediomedial nucleus (IM in Fig. 5A).

The perirotundic (deeper) portion of the intergeniculate leaflet formation contains moderately CB-IR neurons and neuropil (IGL; Fig. 5D), whereas more superficial parts of the IGL are negative.

The medial nucleus appears rostrally in the ventral tier of the dorsal thalamus (adjacent to the zona limitans intrathalamica); it has a strongly CB-IR neuropil, which likewise contains CB-IR neurons (M; Fig. 5A,C,D). More caudally, the medial nucleus is substituted within the ventral tier by the posteromedial nucleus, which also shows a massively CB-IR cell population and an even more intensely CB-immunoreactive neuropil (PM; Fig. 5A,C,E). The PM in its turn is substituted caudally by the caudomedial nucleus, an area which is similar to the medial nucleus in CB preparations, but lies at the boundary with the pretectum (CM; Fig. 5A,C). Ventrolateral to these medially lying nuclei, which jointly form a periventricular stratum, there appears an intermediate mantle region with abundant CB-IR neurons and neuropil, which we have named the posterolateral nucleus (PL; Fig. 5E). This nucleus occupies an intermediate radial position and approaches laterally the superficial ventral tier derivatives, where the dorsal thalamus expands again in surface extent. One of these superficial ventral tier components is the nucleus Z, which lies interstitially within the toromedial tract and has a number of moderately CB-IR neurons (Z; Fig. 5E,F).

Calretinin. In the dorsal tier, calretinin appears in the neuropil and cells of the SHm (Fig. 4D). The subjacent dorsal part of the dorsomedial nucleus, or DM nucleus proper, displays the highest CR-immunoreactivity in the thalamus, present in both neurons and neuropil (DM; Fig. 6A–C). The anterior dorsolateral nucleus is largely negative, but contains weakly CR-IR neurons medially, at its boundary with the DM (DLA; Fig. 6B). In contrast, there is a caudal region, lying behind the typical DLA and medial to the DLP, which shows abundant CR-IR neurons and neuropil; we name this region the caudal dorsolateral nucleus (DLC; Fig. 6C). The dorsal geniculate nucleus contains some barely distinguishable positive neurons in its cell plate and an immunoreactive neuropil (not shown).

In the middle tier, the core of nucleus rotundus appears largely immunonegative for CR (Rd, Ri, Rv; Fig. 6A,C). However, its ventral region has a few weakly immunoreactive neurons (Rv; Fig. 6A,C) and a number of neurons and the neuropil of the three rotundic shell regions are strongly CR-IR (RSp, RSv, RSa; Fig. 6A,C,D). Caudally, the posterior dorsolateral nucleus also contains some immunoreactive neurons (DLP; Fig. 6A,C). The periventricular stratum of the middle tier, the intermediomedial nucleus, found strictly medial to nucleus rotundus, appears also strongly CR-IR (IM; Fig. 6C). The perirotundic, deep part of the intergeniculate leaflet formation also contains a subpopulation of CR-IR neurons (IGL; Fig. 6C,D).

In the ventral tier, the medial and caudomedial thalamic nuclei display a number of CR-IR neurons embedded in a moderately immunoreactive neuropil (M, CM; Fig. 6A,C). Weakly labeled CR-IR neurons appear in the posteromedial nucleus (PM; Fig. 6D). Numerous CR-IR neurons were also found within the posterior nucleus of the ventral supraoptic commissure (PCSV; Fig. 6E).

Parvalbumin. Parvalbumin immunolabeling is wholly absent in both DM and DLA/DLC nuclei of the dorsal tier, whereas the laterally adjacent GD displays a number of strongly immunoreactive neurons, particularly in its superficial neuropil-rich zone (Fig. 7A). In the mid-

Fig. 6. Calretinin immunoreactivity in the dorsal thalamus. **A:** Medial sagittal section through the diencephalon showing the dorsoventral arrangement of the neuronal aggregates in the dorsal thalamus. The dorsolmedial nucleus (DM) is the most prominent periventricular calretinin-immunoreactive (CR-IR) structure of the dorsal thalamus. The boundaries of the ventral thalamus (VT), dorsal thalamus, and the pretectum (PT) are marked by dotted lines. Asterisk marks the CR-IR population of the periventricular stratum fibrosum of the ventral thalamus. **B:** Detail of the dorsal tier in frontal section. CR-IR neurons can be observed in the dorsomedial (DM) and dorsolateral anterior (DLA) nuclei. **C:** The dorsal tier contains the CR-IR dorsolateral caudal nucleus (DLC). The middle tier contains the rotundus core (R; d, i, v, dorsal, intermediate, and ventral parts, respectively), almost immunonegative, surrounded by the anterior rotundic shell and several other CR-IR nuclei (Rsa, IM, DM, IGL, M). Boundaries with the PT and VT are marked by dotted lines. **D:** At a more caudal level, passing through the caudal pole of the middle tier, the posterior and ventral rotundic shell nuclei are CR-IR (RSp, RSv), as well as the posteromedial nucleus (PM) and the intergeniculate leaflet formation (IGL). **E:** Frontal section of the thalamus at the level of the posterior nucleus of the ventral supraoptic commissure (PCSV), a cell mass in the superficial part of the ventral tier, intercalated between the PT and the retromammillary region (RM). Scale bars = 200 μm in A; 100 μm in B–E.

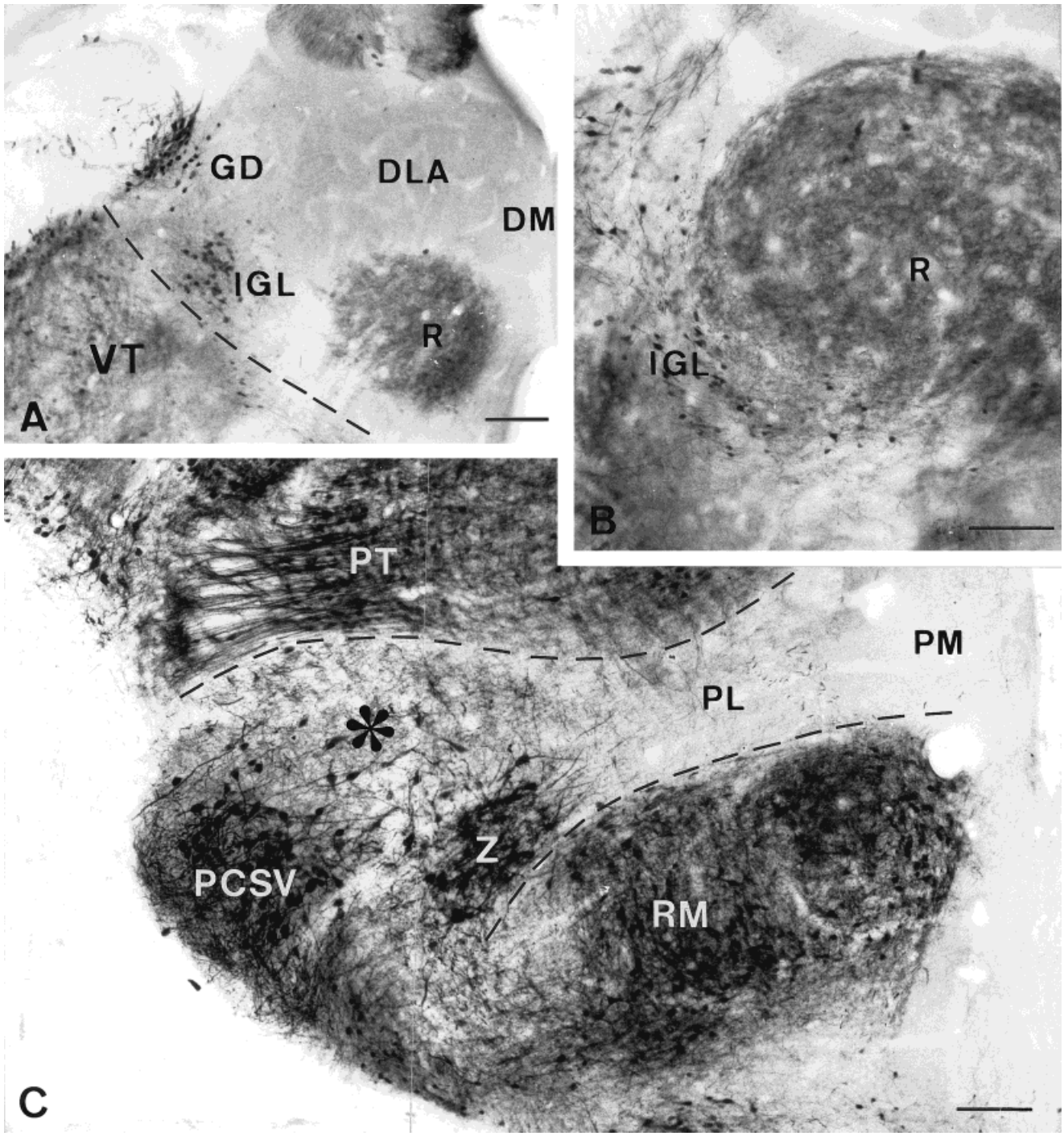

Fig. 7. Parvalbumin immunoreactivity in frontal sections of the dorsal thalamus. **A:** Dorsal and middle tier regions. All dorsal tier nuclei lack parvalbumin (PV) immunoreactivity, whereas in the middle tier, the rotundus nucleus (R) shows a dense PV-IR neuropil. The intergeniculate leaflet formation (IGL) and the dorsal geniculate (GD) display PV-IR neurons. The boundary between dorsal thalamus and ventral thalamus is marked by a dashed line. **B:** Detail of the immunoreactive neuropil in the nucleus rotundus (R). **C:** Photomontage of the caudal region of the dorsal thalamus at the level of the posteromedial and posterolateral nuclei (PM, PL). Interprosomeric limits are marked by dashed lines. The ventral tier displays superficially two intensely PV-IR cellular masses, the nucleus Z and the posterior nucleus of the ventral supraoptic commissure (PCSV). The asterisk labels a neighboring distinct area which is tentatively compared to the avian nucleus ansae lenticularis posterioris. Overlying the ventral tier, appears the intensely PV-IR pretectum (PT; compare Fig. 10). The retromammillary region (RM) displays also a strong immunoreactivity. Scale bars = 100 μm.

dle tier, the neuropil of nucleus rotundus is intensely immunostained (particularly medially), but PV-IR neurons are absent (Fig. 3F, not labeled; R; Fig. 7A,B). In the ventral tier, intense PV-immunoreactivity appears in the large neurons of the nucleus Z, as well as in neurons in the posterior nucleus of the ventral supraoptic commissure (Z, PCSV; Fig. 7C). Caudally adjacent to these nuclei there is a moderately PV-IR neuropil which contains a few strongly positive neurons (asterisk; Fig. 7C). This field touches the boundary with the pretectum and virtually occupies a position identical with that of the avian nucleus ansae lenticularis posterior (see Discussion). The whole intergeniculate leaflet formation contains abundant PV-IR neurons (IGL; Fig. 7A,B). The interstitial nucleus of the optic tract (not shown; see Puelles et al., 1991) represents a neuronal group placed very superficially, next to, or intermixed with fibers of the optic tract.

Ventral thalamus

The ventral thalamus of sauropsids has a reduced extent at the ventricle, due to embryonic compaction, fusion, and resorption of the lips of the transient pseudosulcus parencephalicus, the primitive neuromeric ventricular cavity of p3 (Rendahl, 1924; Kuhlenbeck, 1973; Martínez-de-la-Torre, 1985). However, this alar domain expands considerably superficially (VT; Fig. 3B,D,F; see also Martinez-de-la-Torre, 1985). The periventricular stratum is constituted by the so-called dorsolateral hypothalamic nucleus (not really an hypothalamic element, according to our prosomeric interpretation; zona incerta might be a more appropriate name), plus a cell-poor periventricular stratum fibrosum (DLH; Fig. 2A–C). A zona incerta can be identified ventrally with tyrosine-hydroxylase immunohistochemistry (not shown here; see Medina et al., 1994; Puelles and Medina, 1994). All other ventral thalamic populations occupy either intermediate loci (area intercalata, area triangularis, ventromedial nucleus; AI, AT, VM; Fig. 2A–C) or more superficial positions in the mantle (ventrolateral nucleus, ventral geniculate, lateral suprachiasmatic nucleus, nucleus ovalis; VL, GV, SCL, O; Fig. 2A–C).

Calbindin. Most of the scarce CB-IR cells in the ventral thalamus are located in the intermediate or periventricular regions of the mantle. CB-IR neurons are present in the ventromedial nucleus, extending partially dorsalwards into the overlying area triangularis (AT, VM; Fig. 8A,B; see also Fig. 3B). In VM, the CB-IR cells are embedded among the stained fibers of the dorsal peduncle of the lateral forebrain bundle, which add to the neuropil staining. A few CB-IR neurons were found in the periventricular stratum fibrosum of the ventral thalamus, deep to the dorsolateral hypothalamic nucleus; this area contains a distinct patch of CB-IR neuropil, whereas the DLH shows virtually no immunoreactive cells and a palely stained neuropile (Figs. 2B, 5D, 8A,B). At the superficial, expanded region of the ventral thalamus, some neurons in the ventrolateral nucleus are weakly calbindin-immunopositive, whereas the ventral geniculate nucleus lacks such cells (Figs. 2B, 8B). In contrast, the dorsally located nucleus ovalis presents CB-immunoreactive neurons in its lateral neuropil, which is also moderately immunoreactive (O; Fig. 8A).

Calretinin. Calretinin-immunoreactive neurons are largely restricted to the periventricular stratum fibrosum of the ventral thalamus, deep to the dorsolateral hypothalamic nucleus (Figs. 2D, 8C). We observed a number of CR-IR neurons along the whole dorsoventral extent of this stratum, which are best seen in parasagittal sections; note that this p3 population seems to expand dorsally (asterisk in Fig. 6A), where it appears intercalated between the dorsomedial nucleus of the dorsal thalamus (in p2) and the eminentia thalami and bed nucleus of the stria medullaris (in p4). The remaining cell groups of the ventral thalamus lack calretinin- immunoreactive neurons, with the exception of the superficially located nucleus ovalis, in the cell plate of which a few weakly stained neurons were found (Fig. 8C). In addition, the ventral geniculate nucleus shows a moderately CR-IR neuropil in its superficial plexiform stratum (compare Figs. 2C and 3D). At intermediate dorsoventral levels of the diencephalon, the CR-immunonegative neuropile of the ventral thalamus can be used to identify p3 (intercalated between CR-positive p2 and p4 areas) in sagittal sections (Fig. 3C).

Parvalbumin. As can be seen in transverse sections (Fig. 3F), parvalbumin labeling is preferentially found in the superficial and periventricular strata of the ventral thalamus; this marker provides interesting contrast to calretinin and calbindin labeling. Numerous PV-IR neurons are present within a moderately to strongly PV-IR neuropile both in the lateral plexiform stratum and in the cell plate of the ventral geniculate nucleus (GV; Figs. 3F, 8D). Deep to GV, the intercalate area (Diaz et al., 1994) shows sparser PV-IR neurons and a pale-staining neuropile (AI; Figs. 3E,F, 8D). A number of neurons in the ventrolateral and lateral suprachiasmatic nuclei are also parvalbumin-immunoreactive (VL, SCL; Fig. 8D). Whereas the VM is PV-negative (Fig. 8D), the DLH shows a PV-IR cell population (unlabeled; Fig. 3F). The periventricular stratum fibrosum shows only background staining.

Pretectum

The pretectal region can be subdivided into three nearly transverse sectors, identified as commissural, juxtacommissural, and precommissural sectors, respectively (Martinez-de-la-Torre, 1985; Medina et al., 1992, 1993; Puelles et al., 1996; Pombal and Puelles, 1999; Redies et al., 2000; Yoon et al., 2000). The commissural sector is caudalmost and contains at the periventricular level the posterior commissure and its interstitial nuclei, as well as the subcommissural organ and underlying part of the periventricular stratum fibrosum. The medial pretectal, principal pretectal, and subpretectal nuclei jointly form the intermediate mantle stratum of the commissural pretectum, whereas the posterodorsal nucleus appears in this subdivision dorsally. This sector limits caudally with the mesencephalic griseum tectale. The intermediate, or juxtacommissural, pretectal sector consists of medial and lateral juxtacommissural nuclei (found at deep and intermediate radial levels, respectively), plus the external pretectal nucleus, superficially (the latter is also confusingly known as "lentiform mesencephalic nucleus," though it clearly develops inside the pretectum). The precommissural sector contains a periventricular (periacueductal) gray stratum, the principal precommissural nucleus at intermediate levels, and the precommissural superficial nucleus, or "pretectal geniculate nucleus," superficially (Figs. 2D, 10).

Calbindin. The pretectum is the alar region of the diencephalon showing less calbindin immunoreactivity (Fig. 3A,B). CB-IR neurons are largely restricted to the medial and the lateral juxtacommissural nuclei, whose interstitial neuropiles are devoid of label; nevertheless,

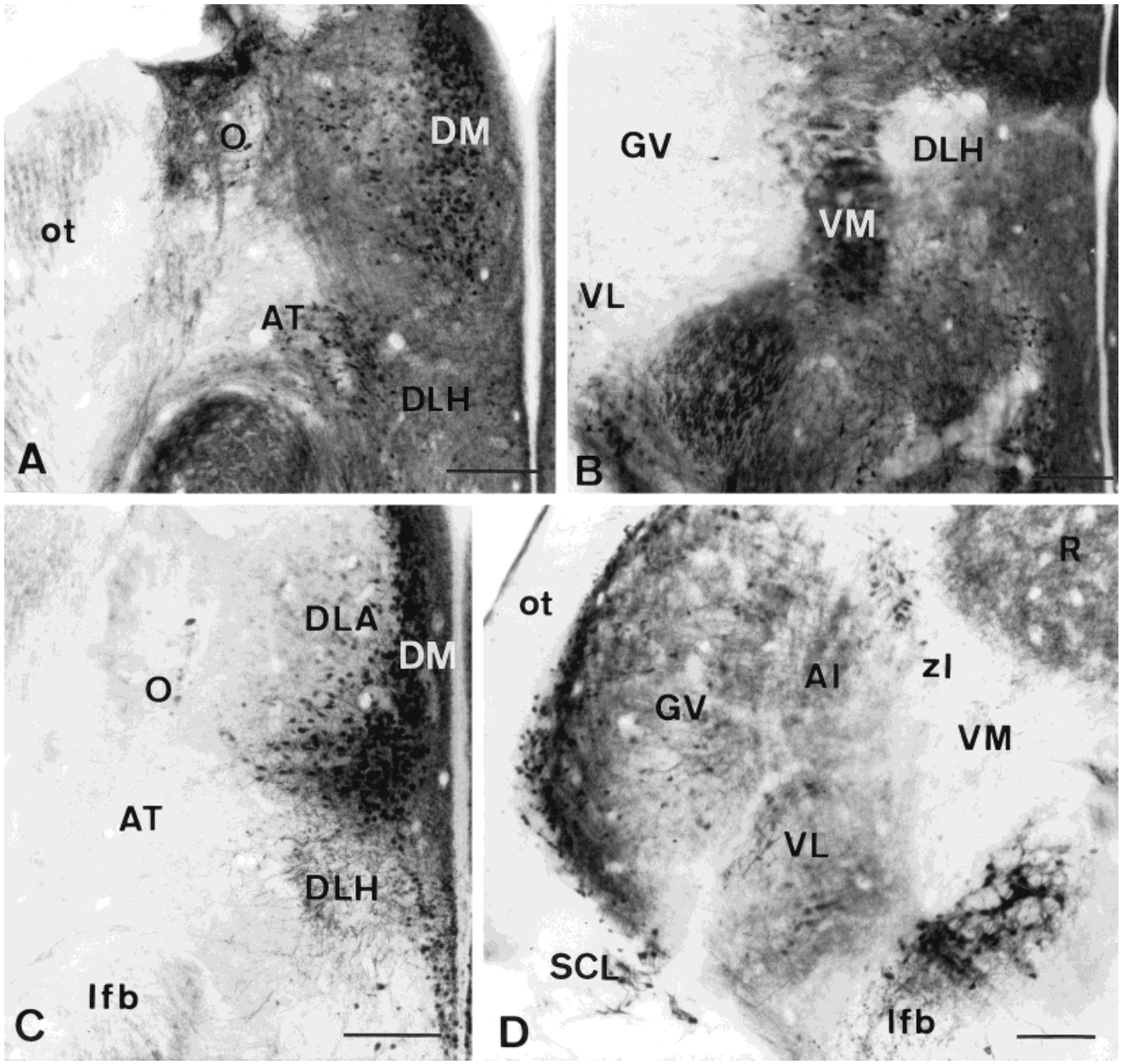

Fig. 8. Calcium-binding proteins in the ventral thalamus. **A,B:** Frontal sections through the diencephalon, immunostained for calbindin. The main calbindin-D28k-immunoreactive (CB-IR) ventral thalamic nuclei (O, AT, VM) are marked. **C:** Calretinin immunoreactivity. The periventricular stratum fibrosum contains abundant calretinin-immunoreactive (CR-IR) neurons. **D:** Parvalbumin immunostaining in lateral ventral thalamic nuclei (GV, VL, AI, SCL). Most PV-IR grisea are located superficially; note the presence of numerous immunoreactive neurons in the neuropil of the ventral geniculate nucleus (GV). The PV-IR supra- or entopeduncular neurons in relationship with the lateral forebrain bundle (lfb) are interpreted as lying outside the ventral thalamus. Scale bars = 125 μm in A,B; 100 μm in C,D.

the lateral juxtacommissural nucleus has a lateral neuropil at its caudolateral boundary with the principal pretectal and subpretectal nuclei, where it displays a moderate CB immunoreaction (JCM, JCL, Fig. 9A). The medial pretectal nucleus shows a weakly CB-IR neuropil, which is continuous ventrolaterally with a neuropil shell around the principal pretectal/subpretectal complex, but it has no cellular expression (PrM; Fig. 9A). Apart from this, a few lightly stained CB-IR neurons were found in the principal precommisural nucleus (not shown).

Calretinin. Calretinin-immunoreactive neurons are also restricted to a few nuclei in the pretectum. In the superficial juxtacommissural sector, the neurons of the external pretectal nucleus are strongly CR-IR (PE; Fig. 9B). In the precommissural sector, the principal precommisural nucleus displays a number of weakly immuno-

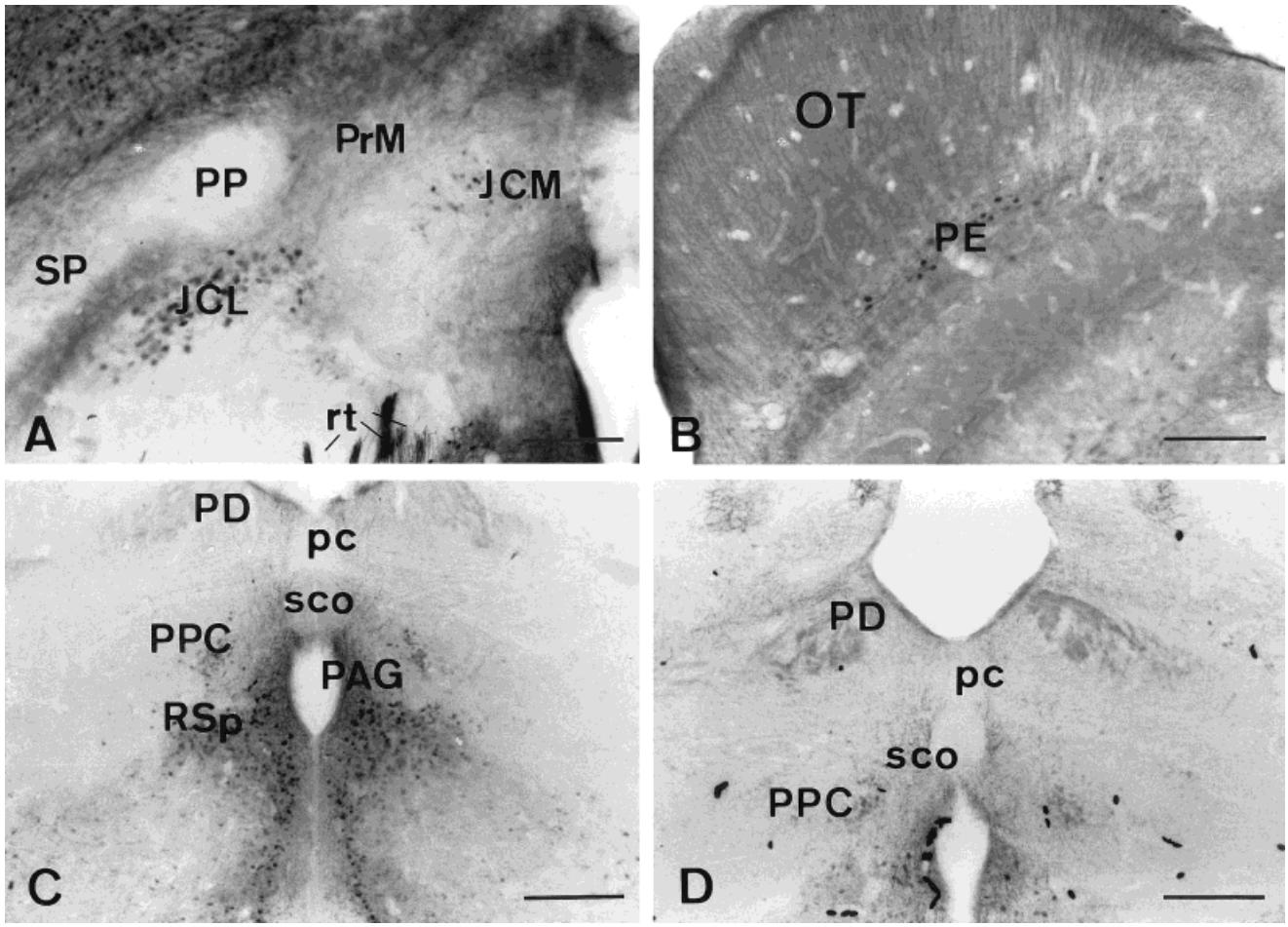

Fig. 9. Calbindin and calretinin immunoreactivity in the pretectum. **A:** Both the medial (JCM) and lateral (JCL) juxtacommissural nuclei display calbindin-immunreactive (CB-IR) cells; note the labeled lateral neuropil of JCL. **B:** Detail of the calretinin-immunoreactive (CR-IR) neurons in the superficially located external pretectal nucleus (PE). **C,D:** Frontal sections through the pretectal region immunostained for calretinin. Some weakly stained neurons appear in the periventricular part of the principal precommissural nucleus (PPC), caudal to the posterior rotundic shell nucleus (RSp). Note also the immunoreactive retinorecipient neuropil of the posterodorsal nucleus (PD). Scale bars = 150 μm.

stained neurons in its deep portion, and the associated periaqueductal gray contains a larger number of CR-IR cells and processes (PPC, PAG; Fig. 9C). In the commissural sector of the pretectum, the superficial, retinorecipient posterodorsal nucleus is noteworthy by its characteristically lobulated CR-IR neuropil (PD; Fig. 9D).

Parvalbumin. In contrast to the two other calcium-binding-proteins, the pretectum is massively parvalbumin-immunoreactive (Fig. 3E,F). In fact, the most intense expression of parvalbumin within the diencephalon is found in the pretectal region. The majority of nuclei in every transverse pretectal sector contain PV-IR neurons (Fig. 10). In the commisural sector, all cellular masses display PV-IR neurons, with the exception of the dorsally placed principal pretectal and posterodorsal nuclei. Abundant PV-IR neurons are found in the subpretectal nucleus, embedded in an immunoreactive neuropil (SP; Fig. 10). Also, both the magnocellular and parvicellular interstitial nuclei of the posterior commissure, as well as the medial pretectal nucleus, display a moderate number of immunoreactive neurons (IPCm, IPCp, PrM; Fig. 10). A packet of fibers in the posterior commissure is PV-IR, but we could not trace their origin (pc; Fig. 10). In the juxtacommissural sector, the lateral juxtacommissural nucleus and its lateral neuropile are massively PV-IR, contrasting with the overlying principal pretectal nucleus, which lacks any immunolabeling (JCL, PP; Fig. 10). The medial juxtacommissural nucleus also contains many PV-IR neurons and a moderately immunopositive neuropil. Some PV-IR neurons likewise appear in the superficially located external pretectal nucleus (JCM, PE; Fig. 10). In the precommissural sector, the periaqueductal gray and the deep part of the PPC only show a few PV-IR fibers; in contrast, the neurons and neuropil of the intermediate stratum of the PPC display an intense-to-moderate parvalbumin immunolabeling (PPC; Fig. 10). The lateral neuropil of the PPC is less immunoreactive and limits with the strongly PV-IR neuronal cell plate of the pretectal geniculate nucleus (GP; Fig. 10). The neurons of GP display a characteristic arrangement of radial immunoreactive dendrites, which extend laterally to contact the optic tract, embedded in the parvalbumin-negative plexiform stratum of the nucleus (compare with Diaz et al., 1999).

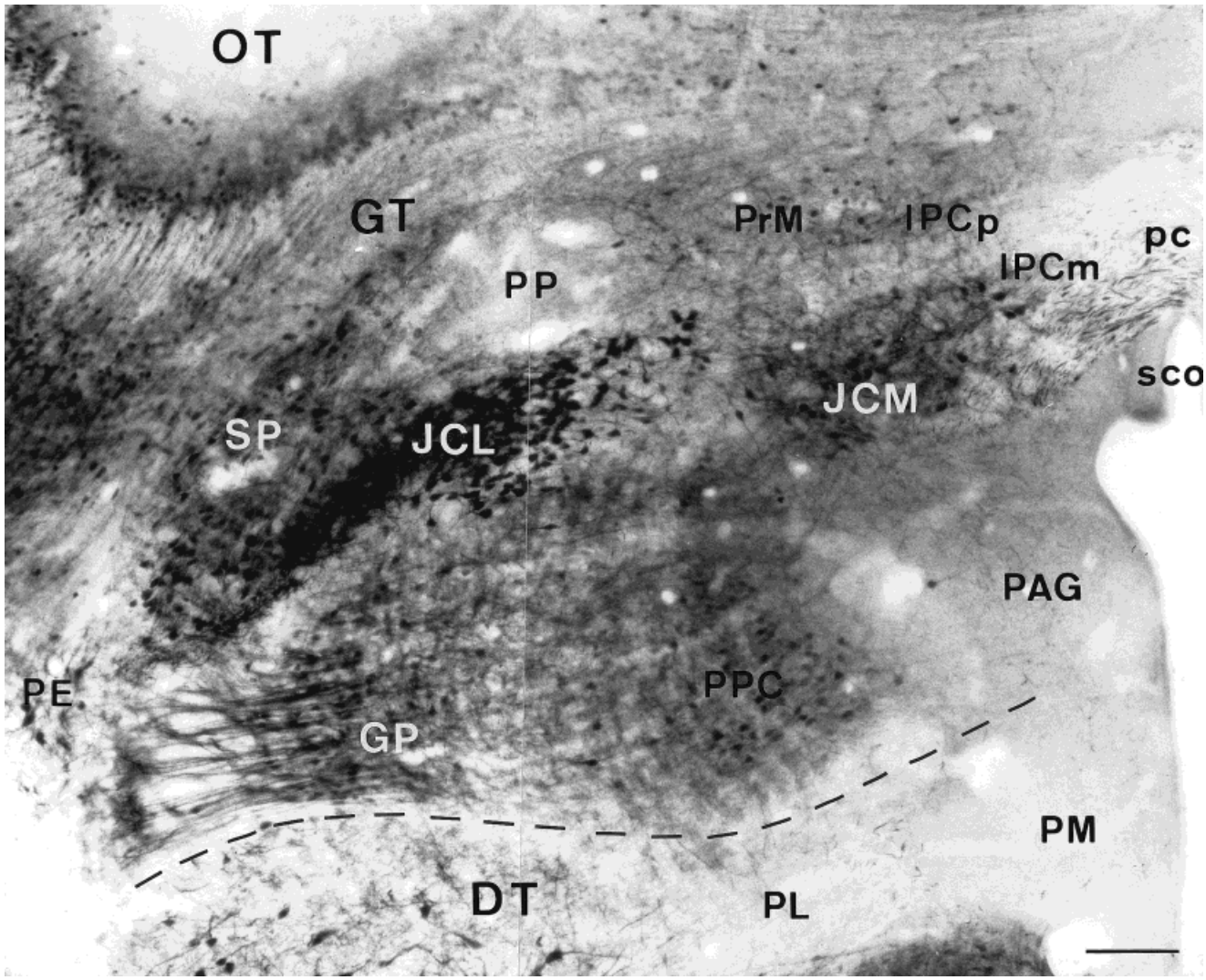

Fig. 10. Photomontage of a frontal section through the pretectal region showing the distribution of parvalbumin. Almost all pretectal nuclei are present in this section and all of them display parvalbumin-immunoreactive (PV-IR) neuronal populations, with the exception of the principal pretectal nucleus (PP). An especially prominent immunoreactivity is found in the lateral juxtacommissural (JCL) and the pretectal geniculate (GP) nuclei. The dorsal thalamus/pretectum limit is marked by a dashed line. Scale bar = 100 μm.

DISCUSSION

We studied the nuclear organization of the lizard diencephalic alar plate, as conceived within the prosomeric paradigm (Puelles, 1995; see also Nieuwenhuys, 1998), by characterizing the differential expression of calbindin, calretinin, and parvalbumin. The respective p1–p3 prosomeric alar domains were identified by reference to observable fiber tracts and other constant landmarks (Fig. 1A,B; Puelles, 1995). Present results in *Psammodromus* show that an extensive CB and CR immunoreaction represents a differential characteristic of the lizard p2 alar plate (dorsal thalamus) versus the p1 and p3 neighboring territories (pretectum, ventral thalamus; Figs. 3, 11; Table 1). Calbindin and calretinin are thus particularly suitable markers for delimiting the dorsal thalamus and epithalamus from neighboring alar forebrain areas, as observed recently in lampreys and frogs (Pombal and Puelles, 1999; Milán and Puelles, 2000), or as can be deduced from mappings performed in the rat or mouse (Puelles et al., 1992; Jacobowitz and Abbott, 1997). Conversely, parvalbumin is more extensively expressed in the pretectum and ventral thalamus than in the dorsal thalamus/epithalamus complex. In the following sections, we will discuss the diencephalic subdivisions thus highlighted in the lizard in comparison to other vertebrates. Some issues concerning terminology and homology raised by the patterns observed will be considered as well.

General comparative comments on calcium-binding proteins as markers in the diencephalon

Calretinin or calbindin represent markers useful for the general distinction of the dorsal thalamus from both pretectum and ventral thalamus in adult anamniote vertebrates. Delineation of pretectal and thalamic centers by

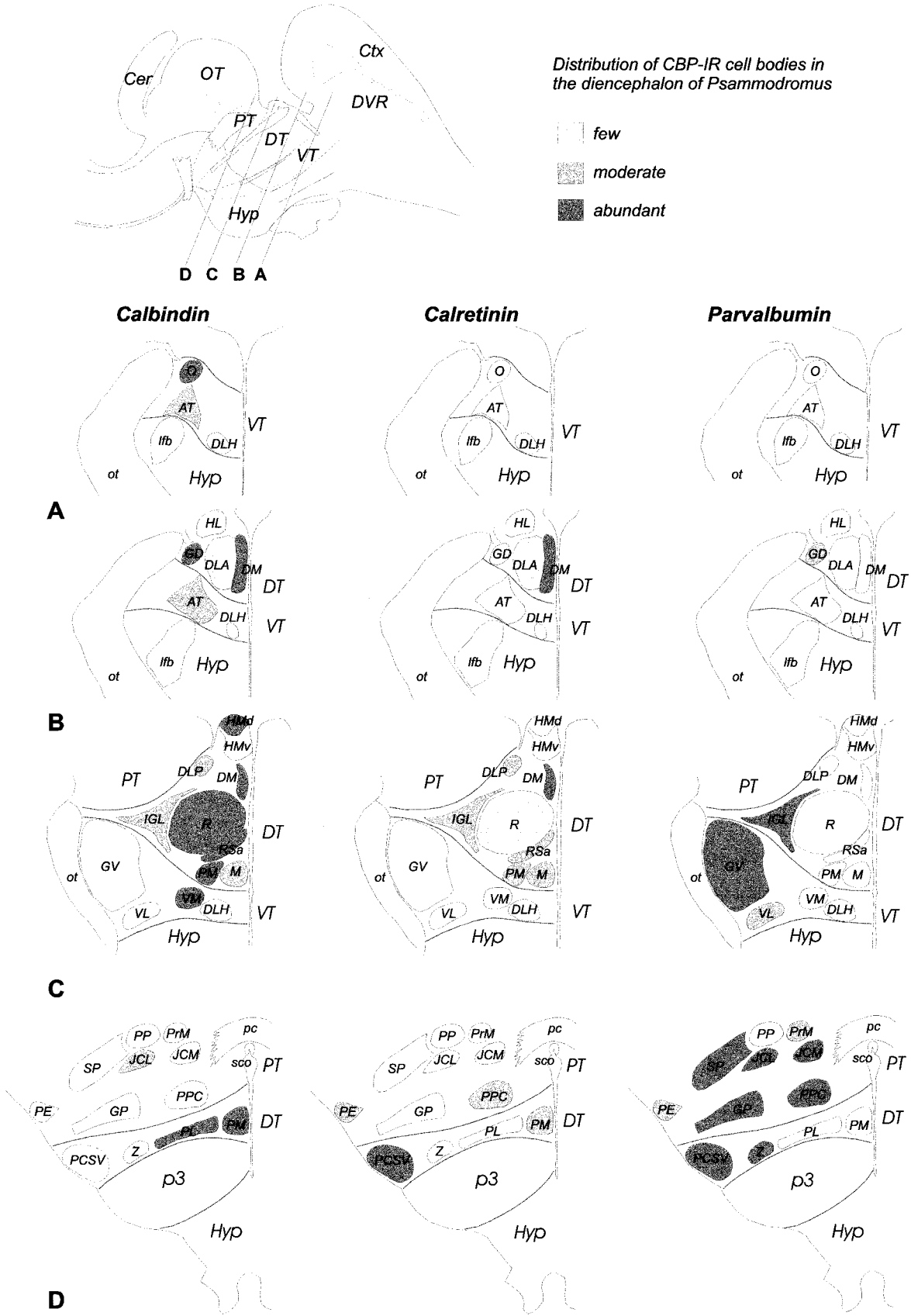

Fig. 11. Summary of the distribution of calcium-binding protein-immunoreactive cell bodies in the diencephalon of *Psammodromus*. Drawings marked from A to D match the same four diencephalic levels showed in Figure 2. Each level of cross-section is marked in the sagittal scheme at the left top of the figure. The boundaries of the pretectum (PT), dorsal thalamus (DT), ventral thalamus (VT), and hypothalamus (Hyp) are marked by dotted lines. The number of calcium-binding protein-imunoreactive (CBP-IR) cell bodies is represented by a three-level gray scale (see Table 1 for comparison).

TABLE 1. The Number of Calcium-Binding Protein Immunoreactive Cell Bodies in Diencephalic Nuclei of *Psammodromus*[1]

	CB-IR[3]	CR-IR	PV-IR
Epithalamus			
Lateral habenular nucleus	+[2]		
Medial habenular nucleus (dorsal)	+++	+	
Dorsal thalamus			
Rostral subhabenular nucleus	++		
Medial subhabenular area	+	+	
Dorsomedial nucleus	+++	+++	
Dorsolateral anterior nucleus	+	+	
Dorsolateral caudal nucleus		++	
Dorsal geniculate nucleus	+++	+	++
Intergeniculate leaflet formation	++	++	+++
Dorsolateral posterior nucleus	++	++	
Intermediomedial nucleus		+++	
Nucleus rotundus	+++	+	
Rotundic shell anterior	+++	++	
Rotundic shell posterior	+++	++	
Rotundic shell ventral		++	
Medial thalamic nucleus	++	++	
Caudomedial nucleus	+++	++	
Posteromedial nucleus	+++	++	
Posterolateral nucleus	+++		
Nucleus Z	+		+++
Posterior nucleus of the commissura supraoptica ventralis		+++	+++
Nucleus ansa lenticularis posterior			+
Ventral thalamus			
Stratum fibrosum periventricular	+	+++	
Dorsolateral hypothalamic nucleus			+
Area intercalata			++
Area triangularis	++		
Ventromedial nucleus	+++		
Lateral suprachiasmatic nucleus			++
Nucleus ovalis	+++	+	
Ventral geniculate nucleus			+++
Ventrolateral nucleus	+		++
Pretectum			
Interstitial nuclei of the posterior commissure			++
Subpretectal nucleus			+++
Medial pretectal nucleus			++
Medial juxtacommissural nucleus	+		+++
Lateral juxtacommissural nucleus	++		+++
External pretectal nucleus		++	++
Periacueductal grey		++	
Principal precommissural nucleus	+	++	+++
Pretectal geniculate nucleus			+++

[1]Only the nuclei displaying immunoreactive cell bodies are listed.
[2]+++, abundant; ++, moderate; +, few.
[3]CB-IR, CR-IR, PV-IR, Calbindin-D28k-, calretinin-, parvalbumin-immunoreactive, respectively.

exclusive use of cytoarchitectonic criteria is difficult in anamniotes. A majority of the dorsal thalamus neurons express calretinin in the lampreys *Lampetra fluviatilis* and *Petromyzon marinus* (Pombal and Puelles, 1999), in *Xenopus* and *Rana* frogs (Milán and Puelles, 2000), and in the urodele *Ambystoma mexicanum* (Puelles and Northcutt, unpublished observations). Many of these neurons occupy a periventricular position, though a variable number of migrated CR-IR cells may appear as well. On the other hand, only a small subset of dorsal thalamic neurons express calbindin in *Xenopus* and *Rana* (Milán and Puelles, 2000). In contrast, periventricular dorsal thalamus neurons in the shark *Scyliorhinus canicula* were found to be massively CB-IR (Rodríguez-Moldes et al., 1990a); it is not known whether CR coexists with CB in this case.

In *Psammodromus*, there seem to be more dorsal thalamic neurons expressing CB than cells expressing CR. Calretinin appears mainly in periventricular cell populations (DM, IM, M nuclei), which usually also express calbindin. Neurons showing exclusively calbindin expression are also more abundant in *Psammodromus* than in frogs (notably in the middle and ventral tier nuclei). However, the DLA nucleus (dorsal tier), which is practically devoid of both markers, shows an anterior subregion richer in CB-positive cells; this can be compared to the rostral part of the frog anterior nucleus (Milán and Puelles, 2000).

Available data on the presence of calcium-binding proteins in the avian diencephalon corroborate a larger presence of both CB and CR in the dorsal thalamus, than in the pretectum and ventral thalamus. Calretinin appears largely restricted to the periventricular stratum and to the intergeniculate leaflet homolog, whereas CB is more extensively distributed in nucleus rotundus, nucleus dorsolateralis posterior, and the periovoidal shell; these represent the avian middle and ventral tiers (Braun, 1990; Aste et al., 1995; De Castro et al., 1998; Redies et al., 2000; Puelles, unpublished observations).

Published accounts on the distribution of these markers in mammals also indicate a restriction of CR, coexpressed with CB, to periventricular dorsal thalamic populations, and a more extensive presence of calbindin in other nuclei (i.e., in the ventromedial, anteromedial, paratenial, centrolateral, posterocentral, and lateral geniculate nuclei; Winsky et al., 1992; Arai et al., 1994; Fortin et al., 1996). Work by Celio and colleagues also underlined an important expression of CB in the posterior/intralaminar complex of the dorsal thalamus and in the shell of the medial geniculate body (Celio, 1990; Séquier et al., 1990). It is remarkable that most of these formations might represent derivatives of the middle and ventral tiers, whereas the ventral, anterior, lateral, and medial nuclear complexes, putative mammalian dorsal tier derivatives, are largely devoid of calcium-binding proteins, as in sauropsids.

On the other hand, parvalbumin is expressed more frequently in pretectal and ventral thalamic neurons than in the dorsal thalamus in both mammals and *Psammodromus* (Celio, 1990; Frassoni et al., 1991; Coveñas et al., 1991; Arai et al., 1994; De Biasi et al., 1994; present results). In fact, the few dorsal thalamic nuclei expressing parvalbumin (e.g., GD, or IGL) may represent a developmentally unitary complex, the anteroventral compartment (Redies et al., 2000; Yoon et al., 2000), which is a specific anteriorly placed neuroepithelial matrix, adjacent to the zona limitans. Previous work suggested the existence in birds of a superficially migrated dorsal thalamic nuclear group which derives in development from a separate, thin matrix area which is placed just behind the zona limitans intrathalamica, and also extends ventrally backwards just over the alar/basal boundary, in a boomerang shape (Rendahl, 1924; Puelles et al., 1991; Martínez et al., 1991). In chick embryos, the migrated cells form a subpial sheet that covers most of the dorsal thalamus. This histogenetically distinct primordium has been corroborated recently by visualization of the genes *Sox-21* (Uchisawa et al., 1999) and *Nkx-2.2* (Puelles et al., 1999), which are differentially expressed in this population during and after its migration to the brain surface. An entirely similar embryonic primordium can be found in lizard embryos (Rendahl, 1924; Martínez-de-la-Torre, 1985).

According to their topography, therefore, the PV-IR populations in the dorsal thalamus probably arise from the anteroventral compartment. Due to the frequent correlation of parvalbumin with GABAergic neurons, it is noteworthy that only anterior portions of the reptilian dorsal thalamus (including the GD homolog) seem to contain GABAergic neurons (Bennis et al., 1991; Rio et al., 1992; Pritz and Stritzel, 1994, Kenigfest et al., 1997) and the

same occurs *mutatis mutandis* in birds (Domenici et al., 1988; Granda and Crossland, 1989).

Regional subdivisions

In addition to the interprosomeric limits, we identified a number of secondary, roughly anteroposterior or dorsoventral subdivisions within the pretectum and dorsal thalamus (see below), in agreement with recent work in the chick (Redies et al., 2000; Yoon et al., 2000). These chemoarchitectonic subdivisions generally are also observable with Nissl staining, and they represent radial subdomains of the respective alar plate regions, which extend from the ventricular surface to the pia. They are postulated to result each from the development of a separate histogenetic area, even though some neuronal populations may migrate from one area into adjacent domains (Puelles, 1995; i.e., the intergeniculate leaflet formation). We will next comment on various structural details in the different diencephalic subregions, referring to wider literature on vertebrates.

Epithalamus. We found that the habenular complex is asymmetric in *Psammodromus*. A singular dorsal part of the left medial habenular nucleus forms a separate nidulus around a neuropil patch; its cells intensely express CB, which is also present in axons entering the left retroflex tract. A comparable asymmetric configuration was observed in the lizards *Uta stansburiana* (Engbretson et al., 1981) and *Gallotia galloti* (Medina et al., 1992). Engbretson et al. (1981) related this asymmetry to an unilateral projection field of the parietal eye. However, a similarly asymmetric CB-IR formation has been described in the medial habenula of the shark *Scyliorhinus canicula* (Rodríguez-Moldes et al., 1990a,b), in the absence of a parietal eye. The lamprey habenula is markedly asymmetric (Pombal and Puelles, 1999), but we lack data on CB expression in this species. Amphibians are known to have an asymmetric left dorsal nidulus in the habenula (Frontera, 1952; Kemali and Braitenberg, 1969; Neary and Northcutt, 1983; Kemali et al., 1990); however, neither CB or CR correlate with this asymmetric portion (Milán and Puelles, 2000). The patterns of calcium-binding proteins found in the habenula of birds and mammals seem to be symmetric (Celio, 1990; Braun, 1990; Jacobowitz and Abbott, 1997; Puelles, unpublished observations). This set of data is limited and may still be inconclusive. Further cladistic comparisons are needed to fully understand these variations and also to resolve whether habenular symmetry evolved independently in birds and mammals.

Dorsal thalamus. The most remarkable structural aspect highlighted by the present observations in the dorsal thalamus is its three-tiered division. This pattern already became apparent in an earlier paper (Diaz et al., 1994), which showed distinct topographic afferent and efferent connections of each tier with portions of the reticular thalamic nucleus. There is evidence for additional hodological specificity of the three dorsal thalamic tiers. Data on thalamo-telencephalic connections in lizards and other reptiles suggest that dorsal tier nuclei tend to receive "lemniscal" afferents and project into cortical telencephalic domains (derivatives of medial and dorsal pallial areas; Hoogland, 1981; Künzle and Schnyder, 1983; Bruce and Butler, 1984a,b; Butler, 1995; Kenigfest et al., 1997; Desfilis et al, 1998). In contrast, the nuclei in the middle and ventral tiers receive strong mesencephalic ("collicular") inputs (tectal, intercollicular, or toral) and project to specific areas in the telencephalic dorsal ventricular ridge (DVR; Pritz, 1974a,b; Pritz and Northcutt, 1980; Balaban and Ulinski, 1981; Belekhova et al., 1983; Bruce and Butler, 1984a,b; Pritz and Stritzel, 1990; Butler, 1995; Guirado et al., 2000). The DVR is a nuclear pallial domain, which has been recently classified into components derived from the lateral pallium and a newly identified component of the vertebrate pallium, the molecularly distinct ventral pallium (equal to the avian neostriatum; Puelles et al., 1999, 2000; see also Striedter, 1997; Smith-Fernández et al., 1998). Neurons in the middle and ventral thalamic tiers project to the ventral pallial portion of the DVR. This hodological pattern led Butler (1995) to distinguish the "lemnothalamus" (roughly equivalent to our dorsal tier, plus DLP) from the "collothalamus" (equal to the rest of our middle and ventral tiers). This topographic-hodologic correlation was previously deduced as well by Martínez-de-la-Torre (1985). The three tiers display characteristic calcium-binding protein expression profiles (Figs. 3, 11; Table 1), which perhaps can be of help in recognizing their homologues in birds (Martínez-de-la-Torre, 1985; Puelles, unpublished observations), and perhaps also in mammals. It is of interest that a similar three-tiered structure can be identified with CR immunochemistry in the lamprey and frog dorsal thalamus (Pombal and Puelles, 1999; Milán and Puelles, 2000).

Dorsal tier. The lizard dorsal tier corresponds topologically to the complex formed by the anterior, lateral anterior, dorsal geniculate, subhabenular, and dorsocaudal nuclei defined in frogs (Puelles et al., 1996; Milán and Puelles, 2000) and to the whole set of "dorsal" suprarotundic nuclei in the avian dorsal thalamus (Martínez-de-la-Torre, 1985; Guillén, 1991; Redies et al., 2000).

The lizard dorsal geniculate nucleus clearly lies at the surface of the dorsal tier, and topographically corresponds to the dorsolateral anterior nucleus pars lateralis and DLA parts of the avian principal optic complex (Dubbeldam, 1998). A somatosensory projection field was found recently in the reptilian DLA (Künzle and Schnyder, 1983; Desfilis et al., 1998), which seems comparable to the avian dorsalis intermedius ventralis anterior nucleus (Wild, 1987a; Funke, 1989; Korzeniewska and Güntürkün, 1990). A viscerosensory thalamocortical relay has been described as well in the avian dorsal tier (Wild, 1987b; Karten et al., 1973). These data suggest the existence in sauropsids of a common set of subnuclei or areas of the dorsal tier complex, which are dedicated to the relay of specific sensory data to parts of the dorsal pallium, as commented above.

Traditionally, the avian dorsolateral posterior nucleus is affiliated with the dorsal tier nuclei (thus the prefix "dorso-"), although diverse data from Puelles' lab have indicated it should be classified in the middle tier (Martínez-de-la-Torre, 1985; Guillén, 1991; Redies et al., 2000), as we have done here with the lizard counterpart. Note that in birds, this nucleus does not project to the telencephalic Wulst, but to the DVR, as is characteristic of middle and ventral tier elements (Gamlin and Cohen, 1986; Wild, 1987a; Funke, 1989). Finally, as regards comparison with mammals, Guillén (1991) proposed that the avian dorsal tier was a field homologue of the largest part of the mammalian dorsal thalamus (i.e., including the medial, anterior, lateral, and ventral nuclear groups, plus the lateral geniculate nucleus) and the same may be

stated of the minimally subdivided lizard dorsal tier, which is clearly less developed than the avian one.

Middle tier. The prominent nucleus rotundus of *Psammodromus* shows abundant CB-IR neurons and several subdivisions, systematized here into dorsal, intermediate, and ventral *core* portions, plus posterior, ventral and anterior *shell* portions. The shell neurons also express CR, whereas the rotundic core is largely CR-negative. The avian nucleus rotundus also displays a number of hodologic and chemoarchitectonic subdivisions (Benowitz and Karten, 1976; Martinez-de-la-Torre et al., 1990; Karten et al., 1997; Redies et al., 2000), whose correspondence with those found in *Psammodromus* are still unclear. These subdivisions in general reflect a complex tectorotundic projection, which probably implies various tectal cell types and distinct target areas inside the rotundus for each of them. Reiner (1994) and Martínez-Marcos et al. (1998) obtained retrograde labeling of different tectal cell types after tracer deposits in the nucleus rotundus of a turtle and a lizard, respectively.

The dorsolateral posterior nucleus, which we tentatively identified in the lizard on the basis of its topographic similarity with the avian homonymous cell group (Redies et al., 2000), is chemoarchitectonically similar to and contiguous with the rotundic complex (see Figs. 4C and 5D). Guillén (1991) also joined the avian DLP nucleus to the nucleus rotundus on the basis of its developmental and neurogenetic pattern. Both rotundus and DLP characteristically show robust CB expression in the lizard (present results) and in the chick (Guillén, 1991; Puelles, unpublished observations).

Ventral tier. This domain is best known by its periventricular components, mainly the auditory medial (or reuniens) nucleus, which receives afferents from the torus semicircularis (Pritz., 1974a; Belekhova et al., 1985; Butler, 1995), and the somatosensory posteromedial/posterocentral complex (Pritz and Northcutt, 1980; Belekhova et al., 1985; Pritz and Stritzel, 1990). This nuclear pattern can be compared straighforwardly with the avian auditory nucleus ovoidalis (Wild, 1987a; Butler, 1995) and somatosensory caudomedial, or retro-ovoidal area (Martínez-de-la-Torre, 1985). These ventral tier nuclei of sauropsids are known to project to caudal parts of the ventral pallium (caudal DVR, caudomedial neostriatum, or field L in birds; review in Dubbeldam, 1998). The mammalian homolog is widely believed to be represented by the medial geniculate body, which generates a projection to the amygdala, primary auditory cortex, and surrounding areas. However, an auditory cortex remains unknown as such in sauropsids. The increased size of the medial geniculate body in mammals, with various subdivisions, and its novel position, migrated to an extreme superficial locus (though clearly within a topologically ventral tier locus within alar p2; see Papez, 1935; Brauth and Reiner, 1991; Puelles et al., 1992) evidences mammalian evolutionary novelty also in this pathway and perhaps concomittantly also in its telencephalic targets. It might be speculated that the homolog of the sauropsidian medial/ovoidal nucleus is represented in mammals by the early-born shell of intralaminar, marginal, peripeduncular, and subparafascicular formations found around the medial geniculate core (see particularly strong CB expression at these loci in the rat in Puelles et al., 1992, and conserved expression of calcitonin gene-related peptide in Brauth and Reiner, 1991); these formations lying around the medial geniculate are known to project, together with the medial subnucleus of the medial geniculate body, to the laterobasal amygdala (reviewed in Voogd et al., 1998), in addition to the auditory cortex (Brauth and Reiner, 1991). The amygdala also contains ventral pallial derivatives, which seem in various aspects comparable to the intermediomedial DVR of reptiles (Crosby, 1917) and the avian caudal neostriatum, areas which receive the projections from the medial/ovoidal nucleus, respectively (Dubbeldam,1998; Puelles et al., 1999). In this scenario, the corticopetal portions of the medial geniculate body (i.e., the ventral, intermediate, and dorsal subnuclei) may be interpreted as structures first emerged in stem mammals.

Other ventral tier nuclei described above occupy a superficial position in the lizard thalamus. The nucleus Z was described in lizard brains (Pritz, 1974a), and its apparent homolog in birds was described recently by Redies et al. (2000). The posterior nucleus of the ventral supraoptic commissure, which is very prominent at the brain surface in reptiles (Martínez-de-la-Torre, 1985; present results), is probably homologous to the avian nucleus of the same name, identifiable by its intense acetylcholinesterase activity (Martínez-de-la-Torre et al., 1990); it occupies a deeper position in birds, due to morphogenetic expansion of the neighboring cell masses related to the optic tract, but it still retains contact with the brain surface under the optic tract (Martínez-de-la-Torre, 1985). This cell group has not been identified in mammals so far. Finally, we described here a distinct caudal cell group within the superficial complex of the dorsal thalamic ventral tier, the posteroinferior nucleus, which occupies an identical relative position as the homonymous nucleus in birds, also known as the posterior nucleus of the ansa lenticularis (Huber and Crosby, 1929; Karten and Dubbeldam, 1973; Brauth et al., 1983). A similar cell population is possibly present in the frog dorsal thalamus (see Discussion in Puelles et al., 1996).

Ventral thalamus. A reticular nucleus has been recently described in the lizard *Gallotia galloti* (Díaz et al., 1994), which projects topographically upon the dorsal thalamus, and seems to be the homolog of the mammalian reticular thalamic nucleus (also a component of the mammalian ventral thalamus). The lizard reticular nucleus consists of three partially overlapping sectors, which correspond to the cell groups conventionally named dorsolateral hypothalamic nucleus, nucleus ventromedialis, and nucleus suprapeduncularis in the literature. The dorsolateral hypothalamic nucleus is reciprocally connected with the dorsal tier of the dorsal thalamus, whereas the ventromedial and suprapeduncular nuclei are reciprocally connected with the middle and ventral tiers of the dorsal thalamus (Díaz et al., 1994).

The distribution of CBP in the ventral thalamus of *Psammodromus* reveals that the lizard reticular complex is also neurochemically heterogeneous, with different sectors (nuclei) expressing a given CBP. Thus, neurons in the periventricular stratum express CR and CB, whereas neurons in the nucleus ventromedialis only express CB, and neurons in the nucleus suprapeduncularis selectively display PV. This distribution pattern of CBP in the ventral thalamus is correlated with a differential immunostaining of the neuropil of the dorsal thalamic nuclei (CR/CB-IR neuropil in nucleus dorsomedialis, CB-IR neuropil throughout the middle and ventral tiers, and PV-IR neuropil only in the middle tier, in nucleus rotundus). Therefore, there exists a specific content of calcium-binding

proteins in the different sectors within the lacertilian reticular thalamic nucleus.

It is interesting to examine the presence of GABA-IR neurons in the ventral thalamus of reptiles, because the mammalian reticular nucleus is GABAergic. In the turtle *Chinemys*, GABA-IR neurons have been observed in the nucleus of the dorsal peduncle of the lateral forebrain bundle (Rio et al., 1992). In the lizard *Ophisaurus* and in *Vipera*, GABA-IR neurons are present in the latter nucleus as well as in nucleus ventrolateralis (Rio et al., 1992). We have some unpublished data on the presence of GABA-IR neurons in the area occupied by the suprapeduncular nucleus and some neighboring entopeduncular neurons inside the lateral forebrain bundle in *Psammodromus*. Pritz and Stritzel (1991, 1993) described numerous PV-IR neurons in the nucleus suprapeduncularis, as found also in the present study. This is consistent with parvalbumin being a marker for GABAergic neurons in the mammalian reticular thalamic nucleus (Frassoni et al., 1991; De Biasi et al., 1994). In *Caiman crocodilus*, the reticular thalamic nucleus contains at least three groups of neurons: glutamic acid decarboxylase (GAD)-IR neurons, PV-IR neurons, and neurons not immunoreactive for either GAD or PV (Pritz, 1995).

On the other hand, neurons expressing different calcium-binding proteins have been described in the mammalian reticular thalamic nucleus. Reticular neurons uniformly express PV (Celio, 1990; Coveñas et al., 1991; Frassoni et al., 1991; Arai et al., 1994). In the thalamus of the guinea pig, all GABA-IR neurons of the reticular nucleus were also intensely PV-IR (De Biasi et al., 1994), but CB-IR neurons have also been described (Winsky et al., 1992), as well as CR-IR neurons (Winsky et al., 1992; Arai et al., 1994; Lizier et al., 1997; Fortin et al., 1998). It is to be noted that CR-IR neurons are preferentially located at the rostral portion of the reticular thalamic nucleus (Lizier et al., 1997), which is the portion of the nucleus projecting to intralaminar and midline nuclei (Velayos et al., 1989; Lizier et al., 1997).

Other ventral thalamic formations distinguished here include the ventral geniculate nucleus, nucleus ovalis, and the ventrolateral nucleus, best visible in PV-immunostained preparations. These are directly comparable to the avian counterparts; nucleus ovalis corresponds to the nucleus lateralis anterior of birds (a mammalian homolog of this formation has not been identified so far). On the basis of relative topography, the sauropsidian ventrolateral nucleus may be compared to the mammalian subgeniculate nucleus.

Pretectum. The pretectum of *Psammodromus* displays a clearcut subdivision into precommissural, juxtacommissural, and commissural regions along the anteroposterior axis, which agrees with previous observations in other lizards (Medina et al., 1992, 1993) and vertebrates (Caballero-Bleda et al., 1992; Puelles et al., 1996; Pombal and Puelles, 1999). The commissural sector contains the retinorecipient nucleus posterodorsalis which is the homolog of the avian nucleus area pretectalis. Apart from nucleus posterodorsalis, the formations of the commissural pretectal region include the tectorecipient pretectal nucleus (its dorsal and ventral parts, i.e., PP and SP in this study, are comparable to the principal/subpretectal parts of birds) and the interstitial parvicellular and magnocellular nuclei of the posterior commissure. The subpretectal nucleus contains dense PV-IR neurons, which agrees with its avian homolog being GABAergic (Domenici et al., 1988; Granda and Crossland, 1989).

The lizard juxtacommissural region contains the nucleus pretectalis externus and the lateral and medial juxtacommissural nuclei. The latter are relay stations for forebrain input to the tectum or the cerebellum, respectively; they correspond to the spiriform nuclear complex of birds (Karten and Finger, 1976; Brauth et al., 1978; Martínez-de-la-Torre, 1985; Medina and Smeets, 1992; Medina et al., 1992, 1993). These nuclei also have been identified in other reptiles and some anamniotes (Martínez-de-la-Torre, 1985; Medina et al., 1992, 1993; Puelles et al., 1996; Pombal and Puelles, 1999; Redies et al., 2000). However, the mammalian homologs are still uncertain (see Caballero-Bleda et al., 1992; Lagares et al., 1994). We showed here their intense expression of PV, absence of CR, and moderate to weak expression of CB (JCL, JCM; Fig.11).

2The nucleus pretectalis externus appears as a superficial transverse band of large and smaller neurons under the optic tract, wedged between the griseum tectale (rostralmost alar midbrain derivative) and the precommissural nucleus geniculatus pretectalis. It represents the joint superficial stratum of the commissural and the juxtacommissural domains of the pretectum, and it contains a mixture of small and larger neurons. Favorable sections show that the deep aspect of this nucleus is continuous with the lateral juxtacommissural nucleus, a pattern which is patent in the pretectum of turtles (Martínez-de-la-Torre, 1985). It clearly corresponds to the avian nucleus pretectalis externus, also in its expression of CR and PV (see Martínez-de-la-Torre, 1985; Puelles et al., 1988, 1991; De Castro et al., 1998). A number of authors confusingly refer to this cell band as "nucleus lentiformis mesencephali."

The intermediate and superficial strata of the precommissural pretectum stand out in PV-IR preparations (Fig.10). The intermediate stratum is formed by the principal precommissural nucleus, which initially used to be identified as "nucleus lentiformis thalami," whereas the superficial stratum contains the nucleus geniculatus pretectalis. These nuclei are directly comparable to the principal precommissural nucleus and the nucleus superficialis synencephali of the avian pretectum (Martínez-de-la-Torre, 1985; Martínez-de-la-Torre et al., 1990; Puelles et al., 1991; Medina et al., 1992, 1993) and they jointly seem to form a field homolog of the anterior pretectal nucleus of mammals (Martínez et al., 1991; Caballero-Bleda et al., 1992).

We propose that the nomenclature of reptilian pretectal nuclei should be unified under the fundamental topological categories of commissural, juxtacommissural, and precommissural nuclei, to avoid the confusion and embryological inconsistency implicit in the classical terminology, which contrasts with the clear topological, cytoarchitectonic, chemoarchitectonic, and hodological comparability noted with the avian pretectum (see Fig. 10 and literature cited above). This should aid comparisons already partly stressed among the different groups of vertebrates (see Puelles et al., 1991, 1996; Pombal and Puelles, 1999).

The reptilian middle and ventral tier nuclei as possible homologs of mammalian nonspecific (posterior and intralaminar) thalamic nuclei

There is suggestive evidence that the sauropsidian R/DLP complex corresponds topologically to the posterior/intralaminar thalamic complex in mammals. The latter, an ill-defined region, bounds with the pretectum caudally, the lemnothalamic or dorsal tier nuclei rostrodorsally (Butler, 1995), and the medial geniculate body (ventral tier) ventrally, as is true of the sauropsidian R/DLP complex. The mammalian posterior/intralaminar complex also contains abundant CB expression (Celio, 1990; Séquier et al., 1990) and correlative periventricular CR expression. The mammalian posterior complex and nearby intralaminar nuclei receive visual and other polymodal afferents from the midbrain and brainstem (Rockel et al., 1972; Harting et al., 1973, 1980; Holstege and Collewijn, 1982; Yamasaki et al., 1986; Bickford and Hall, 1989; Voogd et al., 1998), and apparently partly project to noncortical telencephalic targets mapped within the claustrum and basolateral amygdala (LeVay and Sherk, 1981; Sloniewski, 1983; Kaufman and Rosenquist, 1985; Sloniewski et al., 1986; Carey and Neal, 1986; Price et al., 1987). The telencephalic structures that receive these posterior/ intralaminar thalamic afferents have been conceived as a potential field homolog in mammals of the ventral pallial ("neostriatum") component of the sauropsidian dorsal ventricular ridge, on the basis of hodology, morphological developmental analysis, and gene expression patterns (Holmgren, 1925; Bruce and Neary, 1995; Striedter, 1997, 1998; Smith-Fernández et al., 1998; Puelles et al., 1999, 2000).

This homology hypothesis needs to be contrasted with the widespread hypothesis that the homolog of the sauropsidian nucleus rotundus is the mammalian lateral posterior (LP) nucleus (or inferior pulvinar); this nucleus receives projections from the superficial strata of the superior colliculus, and projects to associative temporal visual cortex (Karten, 1969, 1991, 1997; Butler, 1995). Several lines of thought question this last hypothesis. First, sauropsidian tectorotundal neurons are the earliest born in the tectum (data on the chick: LaVail and Cowan, 1971; Martínez-de-la-Torre et al., 1987). In contrast, the superficial collicular neurons of the rat that project to the LP nucleus are late born at embryonic day (E)15–16. The earliest rat collicular neurons are born at E13 and correspond to the deep strata, whose cells instead project to the posterior/intralaminar thalamic complex (Altman and Bayer, 1981; Bayer and Altman, 1995). The possible assumption that tectorotundic neurons may have changed their neurogenetic chronology, while conserving their hodological properties, is not an easily acceptable one, because it requires multiple drastic changes in the developmental (genetic) control of the clonal structure of the tectum, but cannot be excluded at this stage. Secondly, detailed mappings show that the mammalian LP nucleus is separated from the pretectum by elements of the posterior complex, variously represented by the limitans, suprageniculate, ethmoid, and linearis nuclei described in several mammals (Jones, 1985). Unfortunately, this distinction is lacking in some studies, where the term "LP/pulvinar" is used so that it also includes parts of the posterior complex, thus adding more confusion to this issue (i.e., LeVay and Sherk, 1981). Thirdly, hodological homology arguments are complicated in this case by the fact that the mammalian superior colliculus generates various projections: to posterior and interlaminar nuclei, to LP nucleus/inferior pulvinar, and to lateral geniculate nucleus (reviewed by Voogd et al., 1998). That is, mammals seem to have evolved several tectothalamic neuronal populations; these project upon derivatives of either the middle or dorsal tiers of the dorsal thalamus. We thus tend to regard the mammalian LP/pulvinar complex as an emergent dorsal tier domain (absent or minimally developed in nonmammals), which becomes connected to expanding mammalian associative cortex (Krubitzer, 1995). The "associative" thalamic nuclei in general belong to the dorsal tier or lemnothalamus (Butler, 1995). Conversely, the barely studied posterior thalamic areas intercalated between the pretectum and the LP/pulvinar complex are the major recipients of deep collicular efferents (the best evidence for this appears in Fig. 12 of Holstege and Collewijn, 1982). The late-born tecto-LP connecting population may have been added to an older tectoposterior/tectorotundic one at the separation of mammals from stem amniotes. Such an hypothesis agrees with the observed CB staining patterns.

Sensory dorsal thalamic nuclei in reptiles often have been compared with mammalian sensory nuclei, disregarding their topological differences in terms of allocation to a specific tier, implicit in the distinction of lemnothalamus and collothalamus (Butler, 1994a,b). The reptilian middle/ventral tier nuclei generally project to the striatum and to a pallial structure, the overlying anterior dorsal ventricular ridge (Ulinski, 1983; González et al., 1990; Smeets and González, 1994; Guirado et al., 2000), which was largely viewed in the last two decades as a "functional" equivalent (or even as a homologue) of sensory/associative isocortex of mammals (Karten, 1969, 1991, 1997; ten Donkelaar, 1998). In mammals, the posterior/intralaminar complex is known to project upon the striatum and the pallial claustroamygdaloid complex (Kaufman and Rosenquist, 1985; Sloniewski et al., 1986; Carey and Neal, 1986; review in Price et al., 1987; Reblet and Puelles, unpublished observations). This partly agrees with Holmgren's (1925) hypothesis suggesting that the sauropsidian hypopallium (ADVR plus piriform cortex) is field homologous to the mammalian claustroamygdaloid/piriform complex. The alternative hypothesis forms part of Karten's (1969, 1991, 1997) conception, based on the assumption that thalamorecipient nuclei in the reptilian ADVR can be compared with specific layer IV, layer II/III, or layer V neuronal populations of the mammalian sensory or sensory-associative neocortex, whose immature neurons are postulated to migrate from a DVR-like anlage into selected fields and layers of the developing cortex, conserving their ancient hodological properties. This hypothesis faces several difficulties (see Reiner, 1991; Striedter, 1997; Puelles et al., 2000). In particular, evidence for the massive cell migrations postulated to occur in embryonic mammals, or for the diverse guidance mechanisms that should be involved, is still lacking.

Moreover, contrary to dorsal tier-derived sensory and associative nuclei in mammals, middle and ventral tier sensory nuclei in reptiles lack GABA- and GAD-IR neurons (Bennis et al. 1991; Rio et al., 1992; Pritz and Stritzel, 1994; Kenigfest et al., 1997), as well as PV-IR neurons (present data, see however Pritz and Siadati, 1999),

whereas the same nuclei are "enriched" in CB-IR neurons, a characteristic of "nonspecific" thalamic nuclei in mammals (Celio, 1990; Séquier et al., 1990; Jones, 1998). Another major difference with the dorsal tier-derived sensory nuclei in the mammalian dorsal thalamus is the lack of a reciprocal cortical projection (Lohman and Smeets, 1990; see Pritz, 1995).

All these considerations lead us to suggest that the middle and ventral tiers of the reptilian dorsal thalamus possibly may be homologous as a field to nonspecific or plurimodal posterior/intralaminar thalamic nuclei in mammals. This includes cells in the shell of posterior, intralaminar, and perigeniculate cell populations in the neighborhood of the medial geniculate body, which also distinctly project to the striatum and the claustroamygdaloid complex, apart of the auditory cortex (LeDoux et al., 1985; Brauth and Reiner, 1991).

ACKNOWLEDGMENTS

We thank Jesús Padial for his excellent technical assistance and the two anonymous reviewers for their useful comments.

LITERATURE CITED

Altman J, Bayer SA. 1981. Time of origin of neurons of the rat superior colliculus in relation to other components of the visual and visuomotor pathways. Exp Brain Res 42:424–434.

Andressen C, Blumcke I, Celio MR. 1993. Calcium-binding proteins: selective markers of nerve cells. Cell Tissue Res 271:181–208.

Arai R, Jacobowitz DM, Deura S. 1994. Distribution of calretinin, calbindin-D28k, and parvalbumin in the rat thalamus. Brain Res Bull 33:595–614.

Aste N, Viglietti-Panzica C, Fasolo A, Panzica GC. 1995. Mapping of neurochemical markers in quail central nervous system: VIP- and SP-like immunoreactivity. J Chem Neuroanat 8:87–102.

Balaban CD, Ulinski PS. 1981. Organization of thalamic afferents to anterior dorsal ventricular ridge in turtles. I. Projections of thalamic nuclei. J Comp Neurol 200:95–129.

Bayer SA, Altman J. 1995. Principles of neurogenesis, neuronal migration, and neural circuit formation. In: Paxinos G, editor. The rat nervous system. San Diego: Academic Press. p 1079–1098.

Belekhova MG, Ivazov NI, Safarov KM. 1983. New data on sensory representation in the telencephalon of the lizard (*Ophisaurus apodus*). Zh Evol Biokhim Phiziol 19:478–485.

Belekhova MG, Zharskaja VD, Khachunts AS, Gaidaenko GV, Tumanova NL. 1985. Connections of the mesencephalic, thalamic and telencephalic auditory centers in turtles. Some structural bases for audiosomatic interrelations. J Hirnforsh 26:127–152.

Bennis M, Calas A, Geffard M, Gamrani H. 1991. Distribution of GABA immunoreactive systems in the forebrain and midbrain of the chamaleon. Brain Res Bull 26:891–898.

Benowitz LT, Karten HJ. 1976. Organization of the tectofugal visual pathway in the pigeon: a retrograde transport study. J Comp Neurol 167: 503–520.

Bickford ME, Hall WC. 1989. Collateral projections of predorsal bundle cells of the superior colliculus in the rat. J Comp Neurol 283:86–106.

Braun K. 1990. Calcium-binding proteins in avian and mammalian central nervous system: localization, development and possible functions. Progr Histochem Cytochem 21:1–62.

Brauth SE, Reiner A. 1991. Calcitonin-gene related peptide is an evolutionarly conserved marker within the amniote thalamo-telencephalic auditory pathway. J Comp Neurol 313:227–239.

Brauth SE, Ferguson JL, Kitt CA. 1978. Prosencephalic pathways related to the paleostriatum of the pigeon (*Columba livia*). Brain Res 147:205–221.

Brauth SE, Reiner A, Kitt CA, Karten HJ. 1983. The substance P-containing striatotegmental path in reptiles: an immunohistochemical study. J Comp Neurol 219:305–327.

Brauth SE, Kitt CA, Gerfen CR. 1988. Calcium binding protein in the basal ganglia system of a non-mammalian vertebrate: an immunohistochemical study in the reptile *Caiman crocodilus*. Brain Res 452:367–372.

Bruce LL, Butler AB. 1984a. Telencephalic connections in lizards. I. Projections to cortex. J Comp Neurol 229:585–601.

Bruce LL, Butler AB. 1984b. Telencephalic projections in lizards. II. Projections to anterior dorsal ventricular ridge. J Comp Neurol 229:602–615.

Bruce LL, Neary TJ. 1995. The limbic system of tetrapods: a comparative analysis of cortical and amygdalar populations. Brain Behav Evol 46:224–234.

Butler AB. 1994a. The evolution of the dorsal thalamus of yawed vertebrates, including mammals: cladistic analysis and a new hypothesis. Brain Res Brain Res Rev 19:29–65.

Butler AB. 1994b. The evolution of the dorsal pallium in the telencephalon of amniotes: cladistic analysis and a new hypothesis. Brain Res Brain Res Rev 19:66–101.

Butler AB. 1995. The dorsal thalamus of jawed vertebrates: a comparative viewpoint. Brain Behav Evol 46:209–223.

Butler AB, Northcutt RG. 1973. Architectonic studies of the diencephalon of *Iguana iguana* (Linnaeus). J Comp Neurol 149:439–462.

Caballero-Bleda M, Fernández B, Puelles L. 1992. The pretectal complex of the rabbit: distributions of acetylcholinesterase and reduced nicotinamide adenine dinucleotide diaphorase activities. Acta Anat 144:7–16.

Carey RG, Neal TL. 1986. Reciprocal connections between the claustrum and visual thalamus in the tree shrew (*Tupaia glis*). Brain Res 386: 155–168.

Celio MR. 1990. Calbindin D-28k and parvalbumin in the rat nervous system. Neuroscience 35:375–475.

Celio MR, Heizmann CW. 1981. Calcium-binding protein as a neuronal marker. Nature 293:300–302.

Coveñas R, De León M, Alonso JR, Arévalo R, Lara J, Aijón J. 1991. Distribution of parvalbumin immunoreactivity in the rat thalamus using a monoclonal antibody. Arch Ital Biol 129:199–210.

Crosby EC. 1917. The forebrain of *Alligator mississippiensis*. J Comp Neurol 27:325–403.

Cruce JAF. 1974. A cytoarchitectonic study of the diencephalon of the tegu lizard, *Tupinambis nigropunctatus*. J Comp Neurol 153:215–238.

Dacey DN, Ulinski PS. 1983. Nucleus rotundus in a snake,*Thamnophis sirtalis*: an analysis of a nonretinotopic projection. J Comp Neurol 216:175–191.

Dávila JC, de la Calle A, Gutiérrez A, Megías M, Andreu MJ, Guirado S. 1991. Distribution of neuropeptide Y (NPY) in the cerebral cortex of the lizards *Psammodromus algirus* and *Podarcis hispanica*. Colocalization of NPY, somatostatin and GABA. J Comp Neurol 308:387–408.

Dávila JC, Megías M, de la Calle A, Guirado S. 1993. Subpopulations of GABA neurons containing somatostatin, neuropeptide Y, and parvalbumin in the dorsomedial cortex of the lizard *Psammodromus algirus*. J Comp Neurol 336:161–173.

Dávila JC, Megías M, Andreu MJ, Real MA, Guirado S. 1995. NADPH diaphorase-positive neurons in the lizard hippocampus: a distinct subpopulation of GABAergic interneurons. Hippocampus 5:60–70.

Dávila JC, Padial J, Andreu MJ, Real MA, Guirado S. 1997. Calretinin immunoreactivity in the cerebral cortex of the lizard *Psammodromus algirus*: a light and electron microscopic study. J Comp Neurol 382: 382–393.

Dávila JC, Padial J, Andreu MJ, Guirado S. 1999. Calbindin-D28k in cortical regions of the lizard *Psammodromus algirus*. J Comp Neurol 405:61–74.

De Biasi S, Arcelli P, Spreafico R. 1994. Parvalbumin immunoreactivity in the thalamus of guinea pig: light and electron microscopic correlation with gamma-aminobutyric acid immunoreactivity. J Comp Neurol 348: 556–569.

De Castro F, Cobos I, Puelles L, Martínez S. 1998. Calretinin in pretecto- and olivocerebellar projections in the chick: immunohistochemical and experimental study. J Comp Neurol 397:149–162.

Desfilis E, Font E, García-Verdugo JM. 1998. Trigeminal projections to the dorsal thalamus in a lacertid lizard, *Podarcis hispanica*. Brain Behav Evol 52:99–110.

Díaz C, Puelles L. 1992a. In vitro HRP-labeling of the fasciculus retroflexus in the lizard *Gallotia galloti*. Brain Behav Evol 39:305–311.

Díaz C, Puelles L. 1992b. Afferent connections of the habenular complex in the lizard *Gallotia galloti*. Brain Behav Evol 39:312–324.

Díaz C, Yanes C, Trujillo CM, Puelles L. 1994. The lacertidian reticular thalamic nucleus projects topographically upon the dorsal thalamus: experimental study in *Gallotia galloti*. J Comp Neurol 343:193–208.

Díaz C, Pérez S, L., Martínez-de-la-Torre M, Puelles L. 1999. Diencephalic neuronal populations projecting axons into the basal plate in a lizard (*Gallotia galloti*). Eur J Morphol 37:130–133.

Domenici L, Waldvogel HJ, Matute C, Streit P. 1988. Distribution of GABA-like immunoreactivity in the pigeon brain. Neuroscience 25: 931–950.

Dubbeldam JL. 1998. Birds. In: Nieuwenhuys R, Ten Donkelaar HJ, Nicholson C, editors. The central nervous system of vertebrates. Berlin: Springer. p 1525–1636.

Engbretson GA, Reiner A, Brecha N. 1981. Habenular asymmetry and the central connections of the parietal eye of the lizard. J Comp Neurol 198:155–165.

Fortin M, Asselin M, Parent A. 1996. Calretinin immunoreactivity in the thalamus of the squirrel monkey. J Chem Neuroanat 10:101–117.

Fortin M, Asselin MC, Gould PV, Parent A. 1998. Calretinin-immunoreactive neurons in the human thalamus. Neuroscience 84: 537–548.

Frassoni C, Bentivoglio M, Spreafico R, Sanchez M, Puelles L, Fairen A. 1991. Postnatal development of calbindin and parvalbumin immunoreactivity in the thalamus of the rat. Brain Res Dev Brain Res 58:243–249.

Frontera JG. 1952. A study of the anuran diencephalon. J Comp Neurol 96:51–70.

Funke K. 1989. Somatosensory areas in the telencephalon of the pigeon. II. Spinal pathways and afferent connections. Exp Brain Res 76:620–638.

Gamlin PD, Cohen DH. 1986. A second ascending visual pathway from the optic tectum to the telencephalon in the pigeon (*Columba livia*). J Comp Neurol 250:296–310.

González A, Russchen FT, Lohman AH. 1990. Afferent connections of the striatum and the nucleus accumbens in the lizard *Gekko gecko*. Brain Behav Evol 36:39–58.

Granda RH, Crossland WJ. 1989. GABA-like immunoreactivity of neurons in the chicken diencephalon and mesencephalon. J Comp Neurol 287: 455–469.

Guillén M. 1991. Estructura del epitálamo y complejo superior del tálamo dorsal en aves: estudio embriológico. Doctoral Thesis. Univ. Murcia.

Guirado S, Martínez-García F, Andreu MJ, Dávila JC. 1999. Calcium-binding proteins in the dorsal ventricular ridge of the lizard *Psammodromus algirus*. J Comp Neurol 405:32–44.

Guirado S, Dávila JC, Real MA, Medina L. 2000. Light and electron microscopic evidence for projections from the thalamic nucleus rotundus to targets in the basal ganglia, the dorsal ventricular ridge and the amygdaloid complex in a lizard. J Comp Neurol 424:216–232.

Harting JK, Hall WC, Diamond IT, Martin GF. 1973. Anterograde degeneration study of the superior colliculus in *Tupaia glis*: evidence from a subdivision between superficial and deep layers. J Comp Neurol 148: 361–386.

Harting JK, Huerta MF, Frankfurter AJ, Strominger NL, Royce GJ. 1980. Ascending pathways from the monkey superior colliculus: an autoradiographic analysis. J Comp Neurol 192:853–882.

Hendry SHC, Jones EG, Emson PC, Lawson DEM, Heizmann CW, Streit P. 1989. Two classes of cortical GABA neurons defined by differential calcium binding protein immunoreactivities. Exp Brain Res 7:467–472.

Herguéta S, Lemire M, Pieau C, Ward R, Repérant J. 1993. The embryological development of the primary visual centres in the turtle *Emys orbicularis*. J Anat 183:367–404.

Herrick CJ. 1910. The morphology of the forebrain in amphibia and reptilia. J Comp Neurol 35:413–547.

Herrick CJ. 1948. The brain of the tiger salamander. Chicago: Univ. Chicago Press.

Holmgren N. 1925. Points of view concerning forebrain morphology in higher vertebrates. Acta Zool Stockh 6:413–477.

Holstege G, Collewijn H. 1982. The efferent connections of the nucleus of the optic tract and the superior colliculus in the rabbit. J Comp Neurol 209:139–175.

Hoogland PV. 1981. Telencephalic projections to the eye in *Python reticulatus*. Brain Res 213:173–176.

Huber GC, Crosby EC. 1929. The nuclei and fiber paths of the avian diencephalon, with consideration of the telencephalic and certain mesencephalic centers and connections. J Comp Neurol 48:1–225.

Jacobowitz DM, Abbott LC. 1997. Chemoarchotectonic atlas of the developing mouse brain. Boca Raton: CRC Press.

Jones EG. 1985. The thalamus. New York: Plenum.

Jones EG. 1998. The core and matrix of thalamic organization. Neuroscience 85:331–345.

Jones EG, Hendry SHC. 1989. Differential calcium binding protein immunoreactivity distinguishes classes of relay neurons in monkey thalamic nuclei. Eur J Neurosci 1:222–246.

Karten HJ. 1969. The organization of the avian telencephalon and some speculations on the phylogeny of the amniote telencephalon. Ann N Y Acad Sci 167:164–180.

Karten HJ. 1991. Homology and evolutionary origin of the "neocortex". Brain Behav Evol 38:264–272.

Karten HJ. 1997. Evolutionary developmental biology meets the brain: the origins of mammalian cortex. Proc Natl Acad Sci USA 94:2800–2804.

Karten HJ, Dubbeldam JL. 1973. The organization and projections of the paleostriatal complex in the pigeon (*Columba livia*). J Comp Neurol 148:61–89.

Karten HJ, Finger TE. 1976. A direct thalamo-cerebellar pathway in pigeon and catfish. Brain Res 102:335–338.

Karten HJ, Hodos W, Nauta WJ, Revzin AM. 1973. Neural connections of the "visual wulst" of the avian telencephalon. Experimental studies in the pigeon (*Columba livia*) and owl (*Speotyto cunicularia*). J Comp Neurol 150:253–278.

Karten HJ, Cox K, Mpodozis J. 1997. Two distinct populations of tectal neurons have unique connections within the retinotectorotundal pathway of the pigeon (*Columba livia*). J Comp Neurol 387:449–465.

Kaufman EFS, Rosenquist AC. 1985. Efferent projections of the thalamic intralaminar nuclei in the cat. Brain Res 335:257–279.

Kemali M, Braitenberg V. 1969. Atlas of the frog's brain. Berlin: Springer-Verlag.

Kemali M, Guglielmotti V, Fiorino L. 1990. The asymmetry of the habenular nuclei of female and male frogs in spring and in winter. Brain Res 517:251–255.

Kenigfest NB, Repérant J, Rio J-P, Belekhova MG, Tumanova NL, Ward R, Vesselkin NP, Herbin M, Chkeidze DD, Ozirskaya EV. 1995. Fine-structure of the dorsal lateral geniculate nucleus of the turtle, *Emys orbicularis*: a Golgi, combined HRP tracing and GABA immunocytochemical study. J Comp Neurol 356:595–614.

Kenigfest N, Martínez-Marcos A, Belekhova M, Font C, Desfilis E, Martínez-García F. 1997. A lacertilian dorsal retinorecipient thalamus: a re-investigation in the Old-World lizard *Podarcis hispanica*. Brain Behav Evol 50:313–334.

Korzeniewska E, Gürtünkün O. 1990. Sensory properties and afferents of the N. dorsolateralis posterior thalami of the pigeon. J Comp Neurol 292:457–479.

Krubitzer L. 1995. The organization of neocortex in mammals: are species differences really so different? Trends Neurosci 18:408–417.

Kulenbeck H. 1973. The central nervous system of vertebrates, vol. 3. Part II. Overal morphology pattern. New York: Karger.

Künzle H, Schnyder H. 1983. Do retinal and spinal projections overlap within the turtle thalamus? Neuroscience 10:161–168.

Lagares C, Caballero-Bleda M, Fernández B, Puelles L. 1994. Reciprocal connections between the rabbit suprageniculate pretectal nucleus and the superior colliculus: tracer study with horseradish peroxidase and fluorogold. Vis Neurosci 11:347–353.

LaVail JH, Cowan WM. 1971. The development of the chicken optic tectum. I. Normal morphology and cytoarchitectonic development. Brain Res 28:391–419.

LeDoux JE, Ruggiero DA, Reis DJ. 1985. Projections to the subcortical forebrain from anatomically defined regions of the medial geniculate body of the rat. J Comp Neurol 242:182–213.

LeVay S, Sherk H. 1981. The visual claustrum of the cat. I. Structure and connections. J Neurosci 1:956–980.

Lizier C, Spreafico R, Battaglia G. 1997. Calretinin in the thalamic reticular nucleus of the rat: distribution and relationship with ipsilateral and contralateral efferents. J Comp Neurol 377:217–233.

Lohman AHM, Smeets WJAJ. 1990. The dorsal ventricular ridge and the cortex of reptiles in historical and phylogenetic perspective. In: Finlay BL, Innocenti G, Scheich H, editors. The neocortex. New York: Plenum Press. p 59–74.

Martínez S, Alvarado-Mallart RM, Martínez-de-la-Torre M, Puelles L. 1991. Retinal and tectal connections of embryonic nucleus superficialis

magnocellularis and its mature derivatives in the chick. Anat Embryol (Berl) 183:235–243.

Martínez-de-la-Torre M. 1985. Estructura del mesencéfalo y diencéfalo en aves y reptiles: Aportaciones a una síntesis en la búsqueda de homologías. Doctoral Thesis. Univ. Murcia.

Martínez-de-la-Torre M, Martínez S, Puelles L. 1987. Solitary magnocellular neurons in the avian optic tectum: cytoarchitectonic, histochemical and [3H]thymidine autoradiographic characterization. Neurosci Lett 74:31–36.

Martínez-de-la-Torre M, Martínez S, Puelles L. 1990. Acetylcholinesterase-histochemical differential staining of subdivisions within the nucleus rotundus in the chick. Anat Embryol 181:129–135.

Martínez-Marcos A, Font C, Lanuza E, Martínez-García F. 1998. Ascending projections from the optic tectum in the lizard *Podarcis hispanica*. Vis Neurosci 15:1–19.

Medina L, Smeets WJAJ. 1992. Cholinergic, monoaminergic and peptidergic innervation of the primary visual centers in the brain of the lizards *Gekko gecko* and *Gallotia galloti*. Brain Behav Evol 40:157–181.

Medina L, Martí E, Artero C, Fasolo A, Puelles L. 1992. Distribution of neuropeptide Y-like immunoreactivity in the brain of the lizard *Gallotia galloti*. J Comp Neurol 319:387–405.

Medina L, Smeets WJAJ, Hoogland PV, Puelles L. 1993. Distribution of choline acetyltransferase immunoreactivity in the brain of the lizard *Gallotia galloti*. J Comp Neurol 331:261–285.

Medina L, Puelles L, Smeets WJAJ. 1994. Development of catecholamine systems in the brain of the lizard *Gallotia galloti*. J Comp Neurol 350:41–62.

Milán FJ, Puelles L. 2000. Patterns of calretinin, calbindin and tyrosine-hydroxylase expression are consistent with the prosomeric map of the frog diencephalon. J Comp Neurol 419:96–121.

Neary TJ, Northcutt RG. 1983. Nuclear organization of the bullfrog diencephalon. J Comp Neurol 213:262–278.

Nieuwenhuys R. 1998. Morphogenesis and general structure. In: Nieuwenhuys R, ten Donkelaar HJ, Nicholson C, editors. The central nervous system of vertebrates. Berlin: Springer. p 159–228.

Palmgren A. 1921. Embryological and morphological studies on the midbrain and cerebellum of vertebrates. Acta Zool (Stockh) 1:1–94.

Papez JW. 1935. Thalamus of turtles and thalamic evolution. J Comp Neurol 61:433–475.

Pombal MA, Puelles L. 1999. Prosomeric map of the lamprei forebrain based on calretinin immunocytochemistry, Nissl stain, and ancillary markers. J Comp Neurol 414:391–422.

Price JL, Russchen FT, Amaral DG. 1987. The limbic region. II. The amygdaloid complex. In: Björklund A, Hökfelt T, Swanson LW, editors. Handbook of chemical neuroanatomy. Vol.5. Integrated systems of the CNS, part I. Amsterdam: Elsevier. p 279–388.

Pritz MB. 1974a. Ascending connections of a midbrain auditory area in a crocodile, *Caiman crocodilus*. J Comp Neurol 153:179–198.

Pritz MB. 1974b. Ascending connections of a thalamic auditory area in a crocodile, *Caiman crocodilus*. J Comp Neurol 153:199–213.

Pritz MB. 1995. The thalamus of reptiles and mammals: similarities and differences. Brain Behav Evol 46:197–208.

Pritz MB. 1997. Some morphological features of a visual thalamic nucleus in a reptile: observations on nucleus rotundus in *Caiman crocodilus*. Brain Behav Evol 49:237–248.

Pritz MB, Northcutt RG. 1980. Anatomical evidence for an ascending somatosensory pathway to the telencephalon in crocodiles, *Caiman crocodilus*. Exp Brain Res 40:342–345.

Pritz MB, Stritzel ME. 1986. Percentage of relay and intrinsic neurons in two sensory thalamic nuclei projecting to the non–cortical telencephalon in reptiles, Caiman crocodilus. Brain Res 376:169–174.

Pritz MB, Stritzel ME. 1988. Thalamic nuclei that project to reptilian telencephalon lack GABA and GAD immunoreactive neurons and puncta. Brain Res 457:154–159.

Pritz MB, Stritzel ME. 1990. Thalamic projections from a midbrain somatosensory area in a reptile, *Caiman crocodilus.* Brain Behav Evol 36:1–13.

Pritz MB, Stritzel ME. 1991. Calcium binding protein immunoreactivity in a reptilian thalamic reticular nucleus. Brain Res 554:325–328.

Pritz MB, Stritzel ME. 1992. A second auditory area in the non-cortical telencephalon of a reptile. Brain Res 569:146–151.

Pritz MB, Stritzel ME. 1993. Neuronal subpopulations in a reptilian thalamic reticular nucleus. Neuroreport 4:791–794.

Pritz MB, Stritzel ME. 1994. Glutamic acid decarboxylase immunoreactivity in some dorsal thalamic nuclei in Crocodilia. Neurosci Lett 165: 109–112.

Pritz MB, Siadati A. 1999. Calcium binding protein immunoreactivity in nucleus rotundus in a reptile, *Caiman crocodilus*. Brain Behav Evol 53:277–287.

Puelles L. 1995. A segmental morphological paradigm for understanding vertebrate forebrains. Brain Behav Evol 46:319–337.

Puelles L, Medina L. 1994. Development of neurons expressing tyrosine hydroxylase and dopamine in the chicken brain: A comparative segmental analysis. In: Smeets WJAJ, Reiner A, editors. Phylogeny and development of catecholamine systems in the CNS of vertebrates. Cambrigde: Cambridge University Press. p 381–404.

Puelles L, Martínez S, Martínez-de-la-Torre M. 1988. The locus of optic nerve head representation in the retinotopic projection over nucleus geniculatus lateral ventralis and nucleus griseum tectalis in the chick also lacks a retinal projection. Neurosci Lett 85:35–39.

Puelles L, Guillén M, Martínez-de-la-Torre M. 1991. Observations on the fate of nucleus superficialis magnocellularis of Rendahl in the avian diencephalon, bearing on the organization and nomenclature of neighboring retinorecipient nuclei. Anat Embryol 183:221–233.

Puelles L, Sánchez MP, Spreafico R, Fairén A. 1992. Prenatal development of calbindin immunoreactivity in the dorsal thalamus of the rat. Neuroscience 46:135–147.

Puelles L, Milán FJ, Martínez-de-la-Torre M. 1996. A segmental map of architectonic subdivisions in the diencephalon of the frog *Rana perezi*: acetylcholinesterase-histochemical observations. Brain Behav Evol 47: 279–310.

Puelles L, Kuwana E, Puelles E, Rubenstein JLR. 1999. Comparison of the mammalian and avian telencephalon from the perspective of gene expression data. Eur J Morphol 37:139–150.

Puelles L, Kuwana E, Puelles E, Keleher J, Bulfone A, Rubenstein JLR. 2000. Pallial and subpallial derivatives in the chick and mouse telencephalon, traced by the embryonic expression profiles of the genes Dlx-2, Emx-1, Nkx-2.1, Pax-6 and Tbr-1. J Comp Neurol 424:409–438.

Redies C, Ast M, Nakagawa S, Takeichi M, Martínez-de-la-Torre M, Puelles L. 2000. Morphological fate of diencephalic prosomeres and their subdivisions revealed by mapping cadherin expression. J Comp Neurol. 421:481–514.

Reiner A. 1991. A comparison of neurotransmitter-specific and neuropeptide-specific neuronal cell types present in the dorsal cortex in turtles with those present in the isocortex in mammals: Implications for the evolution of isocortex. Brain Behav Evol 38:53–91.

Reiner A. 1994. Laminar distributions of the cells of origin of ascending and descending tectofugal pathways in turtles: Implications for the evolution of tectal lamination. Brain Behav Evol 43:254–292.

Rendahl H. 1924. Embryologische und morphologische Studien über das Zwischenhirn beim Huhn. Acta Zool Stockh 5:241–344.

Rio J-P, Repérant J, Ward R, Miceli D, Medina M. 1992. Evidence of GABA-immunopositive neurons in the dorsal part of the lateral geniculate nucleus of reptiles: morphological correlates with interneurons. Neuroscience 47:395–407.

Rockel AJ, Heath CJ, Jones EG. 1972. Afferent connections to the diencephalon in the marsupial phalanger and question of sensory convergence in the "posterior group" of the thalamus. J Comp Neurol 145: 105–129.

Rodríguez-Moldes I, Timmermans JP, Adriaensen D, Degroodtlassee MHA, Scheuermann DW, Anadón R. 1990a. Immunohistochemical localization of calbindin-D28K in the brain of a cartilaginous fish, the dogfish (*Scyliorhinus canicula* L). Acta Anat 137:293–302.

Rodríguez-Moldes I, Timmermans JP, Adriaensen D, Degroodtlassee MHA, Scheuermann DW, Anadón R. 1990b. Asymmetric distribution of calbindin-D28K in the ganglia-habenulae of an elasmobranch fish. Anat Embryol 181:389–391.

Senn DG. 1979. Embryonic development of the central nervous system. In: Gans C, Northcutt RG, Ulinski P, editors. Biology of the reptilia, vol IX: neurology A. London: Academic. p 173–244.

Séquier JM, Hunziker W, Andressen C, Celio MR. 1990. Calbindin D-28K protein and messenger-RNA localization in the rat brain. Eur J Neurosci 2:1118–1126.

Shimamura K, Hartigan DJ, Martínez S, Puelles L, Rubenstein JLR. 1995. Longitudinal organization of the anterior neural plate and neural tube. Development 121:3923–3933.

Sloniewski P. 1983. Pretectal connections to the claustrum: an HRP retrograde transport study in cats. Acta Neurobiol Exp (Warsz) 43:165–182.

Sloniewski P, Pilgrim C, Usunoff KG. 1986. Diencephalic and mesencephalic afferents of the rat claustrum. Anat Embryol 173:401–411.

Smeets WJAJ, González A. 1994. Sensorimotor integration in the brain of reptiles. Eur J Morphol 32:299–302.

Smith-Fernández A, Pieau C, Repérant J, Boncinelli E, Wassef M. 1998. Expression of the Emx-1 and Dlx-1 homeobox genes define three molecularly distinct domains in the telencephalon of mouse, chick, turtle and frogs embryos: implications for the evolution of telencephalic subdivisions in amniotes. Development 125:2099–2111.

Striedter GF. 1997. The telencephalon of tetrapods in evolution. Brain Behav Evol 49:179–213.

Striedter GF. 1998. Progress in the study of brain evolution: from speculative theories to testable hypotheses. Anat Rec (New Anat) 253:105–112.

ten Donkelaar HJ. 1998. Reptiles. In: Nieuwenhuys R, ten Donkelaar HJ, Nicholson C, editors. The central nervous system of vertebrates. Berlin: Springer. p 1315–1524.

Uchisawa M, Kamachi Y, Kondoh H. 1999. Two distinct subgroups of Group B Sox genes for transcriptional activators and repressors: their expression during embryonic organogenesis of the chicken. Mech Devel 84:103–120.

Ulinski PS. 1983. Dorsal ventricular ridge: a treatise on forebrain organization in reptiles and birds. New York: John Wiley & Sons, Inc.

Velayos JL, Jiménez-Castellanos JJ, Reinoso-Suárez F. 1989. Topographical organization of the projections from the reticular thalamic nucleus to the intralaminar and medial thalamic nuclei in the cat. J Comp Neurol 279:457–469.

Voogd J, Nieuwenhuys R, van Dongen PAM, Ten Donkelaar HJ. 1998. Mammals. In: Nieuwenhuys R, ten Donkelaar HJ, Nicholson C, editors. The central nervous system of vertebrates. Berlin: Springer. p 1637–2097.

Wild JM. 1987a. Thalamic projections to the paleostriatum and neostriatum in the pigeon (*Columba livia*). Neuroscience 20:305–327.

Wild JM. 1987b. The avian somatosensory system: conexions of regions of body representation in the forebrain of the pigeon. Brain Res 412:205–223.

Winsky L, Montpied P, Arai R, Martin BM, Jacobowitz DM. 1992. Calretinin distribution in the thalamus of the rat: Immunohistochemical and in situ hybridization histochemical analyses. Neuroscience 50:181–196.

Yamasaki DS, Krauthamer GM, Rhoades RW. 1986. Superior collicular projection to intralaminar thalamus in rat. Brain Res 378:223–233.

Yoon M-S, Puelles L, Redies C. 2000. Formation of cadherin-expressing brain nuclei in diencephalic alar plate subdivisions. J Comp Neurol 421:461–480.